T.R.
EGE UNIVERSITY
Graduate School of Applied and Natural Science

SYNTHESIS OF SILICA NANO PARTICLES FROM RICE HUSK ASH AND THEIR CHARACTERIZATIONS

MSc THESIS

Açelya ÇALIŞKAN

Chemical Engineering Department

İzmir
2019

T.R.
EGE UNIVERSITY
Graduate School of Applied and Natural Science

SYNTHESIS OF SILICA NANO PARTICLES FROM RICE HUSK ASH AND THEIR CHARACTERIZATIONS

Açelya ÇALIŞKAN

Supervisor : Prof. Dr. Şerife Şeref HELVACI

Chemical Engineering Department
Chemical Engineering Second Cycle Programme

İzmir
2019

Açelya ÇALIŞKAN tarafından yüksek lisans tezi olarak sunulan 'Pirinç kabuğu külünden silika nano tanelerinin sentezi ve sentezlenen tanelerin karakterizasyonu' başlıklı bu çalışma E.Ü. Lisansüstü Eğitim ve Öğretim Yönetmeliği ile E.Ü. Fen Bilimleri Enstitüsü Eğitim ve Öğretim Yönergesi'nin ilgili hükümleri uyarınca tarafımızdan değerlendirilerek savunmaya değer bulunmuş ve 06.12.2019 tarihinde yapılan tez savunma sınavında aday oybirliği/oyçokluğu ile başarılı bulunmuştur.

Jüri Üyeleri:		**İmza**
Jüri Başkanı	: Prof. Dr. Şerife Ş. HELVACI	
Raportör Üye	: Prof. Dr. Günseli ÖZDEMİR	
Üye	: Prof. Dr. Sacide A. ALTINKAYA	

EGE ÜNİVERSİTESİ FEN BİLİMLERİ ENSTİTÜSÜ

ETİK KURALLARA UYGUNLUK BEYANI

EÜ Lisansüstü Eğitim ve Öğretim Yönetmeliğinin ilgili hükümleri uyarınca Yüksek Lisans Tezi olarak sunduğum 'Pirinç kabuğu külünden silika nano tanelerinin sentezi ve sentezlenen tanelerin karakterizasyonu' başlıklı bu tezin kendi çalışmam olduğunu, sunduğum tüm sonuç, doküman, bilgi ve belgeleri bizzat ve bu tez çalışması kapsamında elde ettiğimi, bu tez çalışmasıyla elde edilmeyen bütün bilgi ve yorumlara atıf yaptığımı ve bunları kaynaklar listesinde usulüne uygun olarak verdiğimi, tez çalışması ve yazımı sırasında patent ve telif haklarını ihlal edici bir davranışımın olmadığını, bu tezin herhangi bir bölümünü bu üniversite veya diğer bir üniversitede başka bir tez çalışması içinde sunmadığımı, bu tezin planlanmasından yazımına kadar bütün safhalarda bilimsel etik kurallarına uygun olarak davrandığımı ve aksinin ortaya çıkması durumunda her türlü yasal sonucu kabul edeceğimi beyan ederim.

06/12/2019

Açelya ÇALIŞKAN

ÖZET

PİRİNÇ KABUĞU KÜLÜNDEN SİLİKA NANO TANELERİNİN SENTEZİ VE SENTEZLENEN TANELERİN KARAKTERİZASYONU

ÇALIŞKAN, Açelya

Yüksek Lisans Tezi, Kimya Mühendisliği Anabilim Dalı

Tez danışmanı: Prof. Dr. Şerife Şeref HELVACI

Aralık 2019, 76 sayfa

Son yıllarda nano taneler yüksek gözeneklilikleri, yüzey alanları, biyo uyumlulukları ve kimyasal koruyuculukları nedeni ile ilaç iletim sistemlerinde sıklıkla kullanılmaktadır. Bu malzemeler yüzey özellikleri sayesinde ilaçların uzun sürede kontrollü salımına olanak sağlamaktadır. İlaç deposu olarak kullanılan nano malzemelerin şekil, boyut, kristal yapı ve yüzey özelikleri ilaç yüklemesi ve kontrollü salımı için önem taşımaktadır.

Projede biyosilika (S) ve fonksiyonelleştirilmiş biyosilika (S-APTES) nano taneleri sentezlenmiş, karakterizasyonları yapılmıştır. Çalışmada silika taneleri pirinç kabuğu külünden elde edilmiş böylece hem tarımsal bir atık değerlendirilmiş, hem de doğal kaynaklar kullanılarak güvenilir, ekonomik ve çevre dostu malzemeler üretilerek literatüre ve ülke ekonomisine katkı sağlanmaya çalışılmıştır. Sentezlenen malzemelerin yükleme ve kontrollü salım profillerinin belirlenebilmesi için daha önce literatürde çalışması pek bulunmayan sefdinir (CFD) seçilmiştir.

SiO_2 taneleri, sahip oldukları yüksek yüzey alanı ve gözeneklilik nedeni ile CFD'nin kontrollü salımı için uygun bir davranış göstermiştir.

Anahtar kelimeler: SiO_2, pirinç kabuğu külü, fonksiyonelleştirilmiş nano silika, ilaç yükleme, kontrollü salım, sefdinir.

ABSTRACT

SYNTHESIS OF SILICA NANO PARTICLES FROM RICE HUSK ASH AND THEIR CHARACTERIZATIONS

ÇALIŞKAN, Açelya

MSc in Chemical Engineering

Supervisor: Prof. Dr. Şerife Şeref HELVACI

December 2019, 76 pages

Recently nanoparticles have been found widely used in drug delivery systems due to their high porosity, surface area, bio-compatibility and chemical protection. These type of materials provide controlled release based on their surface properties. The shape, size, crystalline structure and surface properties of the materials are important properties for drug storage, which are important for drug loading and controlled release.

In the study, pure nano silica (S) and functionalized nano silica particles (S-APTES) were synthesized. Silica particles were extracted from rice husk ash which provided both utilization of agricultural waste and usage of natural sources. The findings of the study will contribute literature and economics since the synthesis method is safe, economic and environmentally friendly. The loading and controlled release were studied using cefdinir (CFD) as a model drug which was not very much studied drug in the literature.

SiO_2 nanoparticles exhibited a suitable behavior in the controlled release of CFD due to its high surface area and porosity.

Key words: SiO_2, rice husk ash, functionalized nano silica, drug loading, controlled release, cefdinir.

PREFACE

The main purpose of this study was converting an agro-chemical waste into a valuable product for pharmaceutical industry. It has been written to fulfill the graduation requirements of Chemical Engineering's Second Cycle Programme at Ege University. I was engaged in researching and writing this dissertation from 2016 to 2019.

The scope of the thesis was determined by my supervisor, Prof. Dr. Şerife Şeref HELVACI. Research Assistant Dr. Huriye Banu YENER taught me how to use all equipment/devices in the laboratory and helped me during the experiments. Both Prof. Dr. Şerife Şeref HELVACI and Research Assistant Dr. Huriye Banu YENER were always ready to answer all the questions I was curious about. In the second year of study, Prof. Dr. Şerife Şeref HELVACI supported me to work at Center of Polymer Systems (CPS) in Tomas Bata University in Zlín through the Erasmus Programme, in order to give me a different vision and perspective. This center is a R&D center affiliated to university, that carries out joint projects with the industry and it has many advanced laboratories. In the laboratories at this center, I had the opportunity to characterize the nano particles I produced with the methods we developed together with Prof. Dr. Şerife Şeref HELVACI and Research Assistant Dr. Huriye Banu YENER. Prof. Dr. Vladimír Sedlařík, the rector of Tomas Bata University in Zlín, guided me during this period. I also met many researchers from all over the world. It was a great experience for me and made me discover the potential of being an international engineer in me.

I gladly present my thesis.

Dedicated to contributing to life.

İZMİR
06/12/2019

Açelya ÇALIŞKAN

TABLE OF CONTENTS

Page

TABLE OF CONTENTS (continued)

Page

LIST OF FIGURES

Figure Page

LIST OF FIGURES (continued)

Figure Page

LIST OF TABLES

Table Page

1. INTRODUCTION

In recent years, nanotechnology has been investigated for many research fields such as biomedical, electronics, food, energy and environment. Controlled drug release practices have gained increasing interest and the quick development in the improved materials has resulted in a significant progress in their development (Trewyn et al., 2008; Kortesuo et al., 2000). The purpose of controlled drug delivery is to administer the requested amount of drug to the relevant areas in the human body and to adjust the drug delivery profile to achieve the best possible therapeutic benefits (De Muth et al., 2011). The advantages of controlled drug delivery systems (Szegedi et al., 2011; Manzano et al., 2008) are improvement of patient convenience, reduction in flunctuation in steady state level, increasing safety margin of high potency drug and reduction in total health care cost.

Particles for the drug release practise are generally designed at the nanoscale level. Nanoporous materials are characterized by large surface area and high pore size and their surface chemical properties can be changed. These properties make them suitable drug delivery carriers.

Among these materials, silica is one of the most studied nano particle in drug delivery applications owing to having mesoporous structure, high specific surface area, large pore volume, adjustable nano pore sizes, nontoxic properties a hydrophilic surface feature and being convenient for surface modification that gives an opportunity of use in advanced drug delivery studies (Chandrasekhar et al., 2003; Herna'ndez et al., 2014).

There are two kinds of sources for silica synthesis: natural or synthetic. The production of materials from natural sources such as agricultural wastes is very common to reduce environmental pollution and cost. Rice husk is one of these agricultural wastes owing to silica content (Azmi et al., 2016; Sankar et al., 2016). Beside the natural sources, synthetic sources are also used for production of silica since this method is relatively easy comparing with synthesis of silica from natural sources. For the production of silica, it was aimed to achieve a production easy and efficient in this study. For this reason, precipitation method were chosen.

Silica nano particles are often used as functionalized form as well. Functinalization effectuates changing hydrophilic property of surface to hydrophobic property so that the hydrophobic material can be compatible with human body for example (Alshatwi et al., 2015; Björkegren et al., 2017; Liou and Yang, 2011). Surface functionalization of silica nano particles were carried out by post-modification method. As functionalization agent, aminopropyl triethoxy silane (APTES) were used. Unfuntionalized and functionalized samples of silica were used for application of drug delivery.

Different types of drugs were studied for release applications in the literature. Among them cefdinir, which chemical structure is given in Figure 1.1, is a cephalorin antibiotic often used for the treatment of community-acquired pneumonia, acute chronic bronchitis, sinusitus and skin-structure infections in adult and paediatric patients (Selvi et al., 2015). In this study, unfunctionalized and functinalized silica nano particles were used in the release of CFD, which was selected as the model drug. The loading and controlled release are defined using CFD which is not very much studied drug in the literature. So, it is thought that this study is going to contribute to the literature.

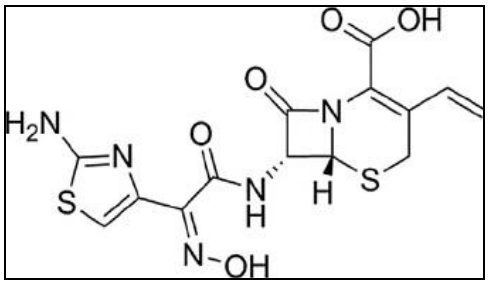

Figure 1.1 Chemical structure of cefdinir.

1.1 Properties of Silica

Silica is the name of a chemical compound consisting of two oxygen and one silicon atom that generally exist in polymorphous forms which are quartz, topaz and amethyst. (Sawe, B.E., 2018). Amorphous silica is more reactive than the crystalline silica. At the same time, amorphous silica has controllable size distribution and high surface area (Chandrasekhar et al., 2003). That is the reason of being preferred in different application fields.

1.2 Sources of Silica

Silica can be synthesized chemically from synthetic materials or obtained from natural sources.

Tetra ethyl ortho silicate (TEOS), whose chemical structure is given in Figure 1.2, is the most commercially used chemical in silica production. The reason of being used of this material is the high size control of the final product and being easy of production. In addition, silanes are used both in production and surface functionalization of silica (Murray et al., 2010).

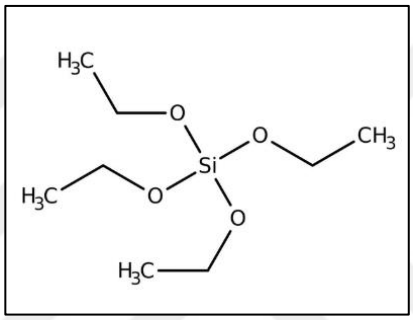

Figure 1.2 Chemical structure of TEOS (Acros organics).

In the past, studies on the production of silica from agricultural waste have used more than one method (Adam et al., 2011; Bergna and Roberts, 2006; Jal et al., 2004). Bark of the plants and the agricultural wastes such as rice husk (RH), sugar cane and peanut shells have become cheap raw material used in silica production. RH contains %71-87 by mass of organic structures such as cellulose and lignin and %13-29 by mass of inorganic elements (Okutani et al., 2009). That is why it is most preferred natural source in silica production.

1.3 Application Fields of Silica

Silica particles in various sizes have many uses. These uses can be customized as catalyst, drug delivery, dental applications, tissue engineering, gene therapy and molecular imaging by reducing the silica particle size to nano level (An et al., 2010; Chen et al., 2017; Gutowska et al., 2001; Liou and Yang. 2011; Yener and Helvacı, 2015; Zulkifli et al., 2013). The nano silica to be produced from rice husk ash

(RHA) is thought to be very useful in some application areas. It can be seen in the literature that the production of nano silica, which is necessary for the production of biomaterials in biological application field, from rice husk ash is so little (Chen et al., 2017). The nano-sized silica granules that will be extracted from rice husk by appropriate method are thought to solve the environmental and economical problems that arise when the old production methods are applied (Tolba et al., 2015).

1.4 Preparation of Sodium Silicate Solution

Firstly the silica is needed to be extracted from the rice husk ash. Silicate solutions are obtained as a results of extraction. Type of silicate changes due to the chemicals used in the extraction process. The extraction process used is called as alkali leaching (Liou and Yang, 2011). In alkali leaching, an alkali solution is used and this alkali solution is generally sodium hydroxide (NaOH) solution. The silica content changes according to the location where the rice husk grows. Conditions (stirring rate, reaction time and temperature) of alkali leaching can vary due to raw material. The reaction occurring during alkali leaching is given in equation below:

$$SiO_{2,RHA}(s) + NaOH(aq) \rightarrow Na_2SiO_3(s) + H_2O(l)$$

The resulting mixture (sodium silicate and ash) is filtered with the aid of filter paper to separate the ash and sodium silicate solution. The solution is kept in the refrigerator.

1.5 Synthesis Methods of Silica

1.5.1 Sol-gel method: Stöber

Two methods are mainly used in silica synthesis: sol-gel and thermal methods. Commonly used sol-gel methods are precipitation and Stöber methods (Zhang et al., 2016; Zulfiqar et al., 2016). Sol-gel methods using different surfactants are called microemulsion method (Le et al., 2013).

In this technique, uniformly dispersed silica particles are obtained by spraying silicon alkoxide dissolved in an alcohol solution. By using sol-gel method with a commercial source such as TEOS, production of silica particle in spherical and micro dimensions is quite common (Stöber and Fink, 1968). In this work, particle diameters range from 0.05 to 3 μm. It has been determined that this method poses a safety problem and creates environmental problems when it was used on a commercial scale due to its usage of heavy chemicals and harmful organic solvents (Dubey et al., 2015; Edrissi et al., 2011; Misran et al., 2013; Park et al., 2002).

1.5.2 Sol-gel method: Precipitation

Precipitation method is second method of the most used production methods (Hieu et al., 2015; Le et al., 2013; Yuvakkumar et al., 2014). This physicochemical method involves two steps: alkali dissolution and acidic precipitation. Acidic chemicals are used to precipitate the rice husk ash solution treated with different alkaline chemicals. In this process, the sensitivity of the silica surface is utilized. At pH=10 and lower, the solubility of the amorphous silica in water is low and its solubility increases with increasing pH. So, the silica is dissolved in alkali and precipitated at a low pH. Silica is then obtained after washing and drying (Liou and Yang, 2011).

Silica syntheses, which are studied intensively today, are mostly carried out by the methods mentioned above. Liu and coworkers (2016) conducted a study of heat treatment and gelation together. In their study, the silica source treated with an alkali chemical was heat treated at 600-900 ^{o}C under atmospheric conditions. They produced silica nano particles in spherical, amorphous structure and submicron dimensions by acid precipitation.

1.5.3 Sol-gel method: Micro-emulsion

In the micro-emulsion process, the reaction medium consists of two phases as oil and water phases. Depending on the solubility of the raw material used, the raw material is distributed in one of these two phases. The starting material is dispersed in the other phase. The reaction starts when the two phases are mixed.

Surface active agents are generally used in this method. The surfactant acts as a nano reactor while surround the materials dispersed in two phases. In this way, the size and shape of the silica can be controlled due to the micelle size formed by the surfactant and the swelling capacity of the micelle formed (Misran et al., 2013). Alkoxy silanes such as TEOS or silicate solutions are also used as raw materials.

1.5.4 Thermal method

In the direct heating method, the rice husk/rice husk ash is directly burned without any preprocessing in this method (James and Rao, 1986; Kapur, 1985; Luan and Chou, 1990; Nakata et al., 1989; Wang and Low, 1990). The percentage of silica purity increases together with the burning of the organic part of the rice husk heat treated under various gases or atmospheric conditions. It was determined in a study that the phase composition and the surface area of silica produced were changed according to the combustion temperature (Kapur, 1985). Chandrasekhar and coworkers (2003) shown that silica particles synthesized is in amorphous structure when calcined in air at 800^{o}C or lower and crystalline structure when calcined at temperatures higher than 900^{o}C.

In some studies pretreatment is used before heating process. Xiong et al. (2009) concluded that the washing of the rice husk with HCl (hydrochloric acid) before the burning process results in a purity (99.5%) and a higher surface area of silica (260 m^2/g). This pretreatment removes all metallic impurities such as Na, K, Ca, Mg, Fe and Cu. After acid pretreatment, carbonization is carried out in air or inert gas atmosphere. In Real and coworkers' study (1996), it has been shown that if acid washing is done prior to incineration, the specific surface area of the silica increases while this pretreatment occurs after incineration, on the contrary. In another study, the rice husk was pre-washed with acid to remove metal impurities in it and then calcined at 700^{o}C and then spherical particles in amorphous structure and average 60 nm size were obtained (Liou et al., 2004).

Treatment can also be done with alkali materials other than acid. Javed and coworkers (2010) used $KMnO_4$ (potassium permanganate) as a pretreatment chemical for preparing high purity amorphous silica and this alkali solution reduced

the cellulose and organic content of the rice husk and acted as an oxidizing agent during thermal decomposition.

Deionized water can be used for pretreatment process as well. A relatively small-sized silica particle was obtained from rice husk which was washed with deionized water and calcined (Shen et al., 2011).

In many studies, it has been figured out that the silica obtained with prepurification processes influences the purity (Alshatwi et al., 2015; Carmona et al., 2013; Palanivelu et al., 2016).

1.5.5 Literature survey on the methods of silica production

The reaction conditions, important parameters and product characteristics for each method are given in Table 1.1 to 1.4.

Table 1.1 Experimental conditions of Stöber method.

Ref.	TEOS (M)	H_2O (M)	NH_3 (M)	Solvent (M)	n_{TEOS}/n_{H2O}	n_{TEOS}/n_{NH3}	Solvent	Temperature (ºC)	Time (h)	Particle size (nm)
Liu et al., 2017	0.47	1.11	0.05	x	0.42	9.32	Ethanol	x	x	20
Ren et al., 2017	0.14	x	2.65	17.12	x	x	Ethanol	60	12	20
Arantes et al., 2012	0.20	x	0.3	17.12	x	0.67	Ethanol	25	24	19
Milly et al., 2010	0.14	2.14	0.32	17.12	0.06	0.42	-	30	0.03	27

Table 1.2 Experimental conditions of precipitation method.

Ref.	Silica source	Pre treatment	Precipitation agent	Post treatment	Results (Size (nm) / Shape)
Mor et. al., 2017	RHA	Alkali Leaching (2 M NaOH / 100 °C / 2 h)	1 N HCl	Drying (50 °C)	5-10 / Spherical agglomerated
Zulfiqar et. al., 2015	RH	Acid leaching (HCl) Calcination (600 °C / 4 h) Alkali leaching (2M NaOH / 2 h)	H_3PO_4	Aging (25- 65 °C / 30 min.)	180-200 / Spherical agglomerated
Vaibhav et.al., 2014	RH	Calcination (900 °C / 7 h) Alkali leaching (1 M NaOH)	3 N H_2SO_4	Aging (12 h) Washing Drying(80ºC / 24 h)	20-40 / Fiber like
Yuvakkumar et. al., 2014	RH	Calcination (700°C / 3 h) Acid leaching (3 M HCl / 1.5 h) Alkali leaching (0.5-2.5 N NaOH / 80°C / 1.5 h)	Conc. H_2SO_4	Calcination (700 and 1100 °C / 3 h)	25 / Spherical agglomerated

Table 1.3 Experimental conditions of micro-emulsion method.

Ref.	Silica source	Surfactant/ Surfactant type	Oil phase	Precipitation agents	Post treatments	Particle size (nm)
Narayanan et al., 2008	Na_2SiO_3 (commercial)	Tween 80 and Span 80 Non-ionic	n-hexane	NH_4HCO_3	Washing (water) Drying (100ºC / 12 h)	1000-10000
Jesionowski et al., 2008	Na_2SiO_3 (commercial)	Rokafenols N3 and N6 Non-ionic	cyclohexane	5 w % HCl	Washing (water/methanol/ethanol) Drying (105 ºC / 48 h)	393
Lee et. al., 2006	Na_2SiO_3 (commercial)	Triton N57 Non-ionic	cyclohexane	$(NH_4)_2SO_4$	Washing (water/acetone) Drying (100 ºC / 24 h)	810
Chattopadhyay and Gupta, 2003	Na_2SiO_3 (commercial)	AOT Anionic	n-heptane or isooctane	Supercritical CO_2	Washing (water) Ultrafiltration	20-800

Table 1.4 Experimental conditions and silica properties synthesized by using thermal methods.

Ref.	Silica source	Pre-treatment		Thermal treatment method	Temperature (ºC)	Time (h)	Results Size (nm)
		Acid leaching	Drying				
Chen et. al., 2017	RH	2.5 w % CH_3COOH, HCl, H_2SO_4	105 ºC, 2 h	Calcination	600, 700, 800, 900	0.5	50
Palanivelu et. al., 2016	RH	10 w % HCl	100 °C, 1 h	Pyrolysis	750	3.0	10-100
Sankar et. al., 2016	RHA	10 w % HCl	150 ºC, 24 h	Calcination	700	2.0	3-10
Alshatwi et. al., 2015	RH	1 N HCl	85 ºC, 5 h	Calcination	500, 600, 700	1.0	100-120
Wang et. al., 2014	RH	5 w % $C_6H_8O_7$	100 ºC, 24 h	Calcination	800	0.5	60
Carmona et. al., 2013	RH	$C_6H_8O_7$, CH_3COOH H_3PO_4	60 ºC, 18 h	Calcination	650	1.0	180-290

1.6 Surface Functionalization of Silica

Silica is used in many different areas, but it is used commonly as a filler or reinforcing additive in advanced composite materials (Rahman et al., 2012). In order to achieve a homogenous distribution with silica and different materials and to turn silica into an effective additive, it can be dispersed uniformly in many different solvents. For this purpose, silica is functionalized by surface modification methods. Generally silanes are used to modification of silica surface (Ayad et al., 2016; Mahmoodi et al., 2011). Silanes have an organofunctional and a hydrolyzable groups in their structure. There is a hydrocarbon chain linking these two groups.

Silanes are commonly called hydrophobic or hydrophilic, depending on the organofunctional group that is in its structure. The silanes commonly used in hydrophilic surface modification of silica are amino, polyethylene oxide and epoxy silanes with hydrophilic functionality. For hydrophobic surface modification, alkyl silanes are often used (Petchu et. al., 2017).

1.6.1 Methods of surface functionalization

Surface functionalization methods basically consists of two groups which are co-condensation (CC) and post functionalization (PF). In the co-condensation method, the modification agent is present in the reaction medium during the synthesis of the silica particle. During the silica particle formation, the functionalizing agent works also in the condensation step with the silica source, resulting the surface modified silica. In the post funcitonalization method, silica is synthesized before the particle functionalization step. The silica is dispersed in the suitable solvent for functionalizing agent, and then the functionalization agent is added to the medium to perform surface functionalization. In some cases, especially where the Stöber method is used, the functionalization agent is added to the reaction medium without removing the silica produced at the end of the reaction. The functionalized particle is obtained after the required time of reaction. In both methods, the excess agent is removed by the help of various washing operations.

1.6.2 Literature survey on surface modification

There are many literature examples in both methods used for surface functionalization of silica. These examples can be seen in Table 1.5.

Table 1.5 Literature survey of surface modification methods.

Ref.	Method	Silica Source	Functionalization agent	Experimental conditions			Area of study
				Temp. (°C)	Time (h)	Medium	
Wang et al., 2016	CC	TEOS	Aminopropyltriethoxy silane	ice-bath	2	Acetonitrile /water	Adsorption
Björkegren et al.,. 2015	PF	Colloidal nano silica particles (commercial)	Methylpolyethyleneglycol silane	25, 70	-	Silica suspension at pH 9	Colloidal stability
Yong et al., 2014	CC	TEOS	Triaminopropyltrimethoxy silane Triisobutyltrimethoxy silane Octyltriethoxy silane	25	18	Ethanol-water	Surface coating and bioanalytical applications.
Lee et al., 2011	PF	TEOS derived silica particles	Methyltriethoxy silane Vinyltrimethoxy silane Triamino(propyl)trimethoxy silane Trimercapto(propyl)trimethoxy silane	40	-	Ethanol-water	Hydrophobicity of different silanes
Park et al., 2009	CC	Na_2SiO_3	Aminopropyltriethoxy silane Mercaptopropyltriethoxy silane Chloropropyltriethoxy silane Pyrrolidine silane	40	1	Water	Catalyst

CC: Con-condensation
PF: Post-funtionalization

1.7 Literature Survey on Drug Loading

The literature survey regarding to drug loading is given in Table 1.6.

Table 1.6 Literature survey of drug loading.

Ref.	Drug	Drug carrier	Drug loading conditions				Drug uptake (w%)
			Drug loading medium	Drug carrier amount (g)	Drug conc. (g/L)	Loading time (h)	
Yılmaz et al., 2016	Flurbiprofen	Silica Trimethylmethoxysilane modified silica	ethanol	-	700	24 24 24 24	27.09 16.96 13.59 9.19
Arean et al., 2013	Cisplatin	Silica Aminopropyltriethoxysilane modified silica Carboxylic acid modifed silica	H_2O	0.0087 0.0614 0.0147	1 1 1	24 24 24	8.7 61.4 14.7
Maria et al., 2012	Cefotaxime Cefuroxime Cefaloxime	Silica Aminopropyltriethoxysilane modified silica Triethoxyvinylsilane modified silica	H_2O	54.4-68.5 54.7 54.6	10.6-10.9/6.82/6.64 10.6-10.9/6.82/6.64 10.6-10.9/6.82/6.64	24 24 24	28.9-40.1/34.0/21.4 27.8/-/- 23.9/-/-
Maria et al., 2012	Irinotecan	Silica Aminopropyltriethoxysilane modified silica Triethoxyvinylsilane modified silica	H_2O	0.1 0.1 0.1	6.6 6.6 6.6	24 48 48	35.8 34.9 36.3
Zhang et al., 2010	Telmisartan	Silica Aminopropyltriethoxysilane modified silica	acetic acid	-	100 100	10 10	48.9/59.1/59.7 50.2
Song et al., 2005	Ibuprofen	Silica	hexane	0.2 0.2	30 30	72 72	25.6/20.6/29.9/37.2 1.7/4.8/6.3/8.2

1.8 Release Kinetics

There are many models for release kinetics. Among them, the featured models are zero order, first order, Higuchi and Korsmeyer-Peppas. The best way to figure out the most convenient model to the release process is to proceed the fit test (Korsmeyer et al., 1983; Liu et al., 2016).

Korsmeyer-Peppas model is generally used to describe release kinetics for polymeric systems. The other model for the release kinetics is Higuchi model. This system describes the release by Fickian diffusion (Dash et al., 2010; Kalu et al., 2007; Kalam et al., 2007).

General function of rate equation is given by equation below:

$$-\frac{dM}{dt} = kM^n$$

By rearranging the equation,

$$\frac{dM}{M^n} = -kdt \tag{1.1}$$

where M is the amount of drug inside the dialysis tubing at a time t and n is the order of the rate equation (Yoo et al., 2003; Singhvi and Singh, 2011; Dash et al., 2010).

By taking n=0, zeroth order rate equation can be obtained as below:

$$dM = -kdt$$

$$\int_{M_0}^{M} dM = -k\int_{0}^{t} dt$$

$$M - M_0 = -kt$$

$$M = M_0 - kt \tag{1.2}$$

By taking n=1, first order rate equation can be obtained as below:

$$\frac{dM}{M} = -kdt$$

$$\int_{M_0}^{M} \frac{dM}{M} = -k \int_{0}^{t} dt$$

$$\ln M - \ln M_0 = -kt$$

$$\ln \frac{M}{M_0} = -kt \qquad (1.3)$$

where M is the amount of drug inside the dialysis tubing at a time t, M_0 is the initial amount of drug inside of the dialysis tube and k is the rate constant.

2. EXPERIMENTAL STUDY

The experimental section consists of four parts, synthesis of silica alcogel from rice husk ash, functionalization of silica alcogel surfaces by APTES, loading of CFD and in-vitro release of CFD, which gives detailed information about these parts.

Firstly the materials used for the synthesis of S and S-APTES nanoparticles were explained. Then the analysis techniques used during the parts were given in detail.

The following part after explaining the materials and analysis techniques used during the experiments contains the parametric study of synthesis of functionalized silica nanoparticles.

The loading method of CFD onto S and S-APTES nanoparticles and the materials used for the loading process were told after the part of production of nanoparticles.

The in-vitro release of CFD from S and S-APTES nanoparticles is the subsequent part of the experimental section. The detailed information about the in-vitro release were given in this section.

2.1 Materials

The raw materials/chemicals utilized in the experiments and some properties of them contaning formula, mission, brand/supplier, molecular weight and density are tabulated in Table 2.1 and chemical structure of some of them are shown in Figure 2.1. In all experiments, double treated water with a pH and conductivity of 5-7 and 1.1 $\mu S\ cm^{-1}$, respectively, was used for the solutions. Except rice husk ash, no pre-treatment was done before using raw materials/chemicals and they were used as they were received. Rice husk ash, which is an output of burning process of rice husk at 700°C for 6 hours under atmospheric conditions, had different sizes of particles so it was used after grinding process.

Table 2.1 Properties of the chemicals/materials used in the experiments.

Materials	**Formula**	**Mission**	**Brand/Supplier**	**Molecular weight (g/mol)**	**Density (g/cm^3)**
Rice husk ash	RHA	Silica source	Erdoğanlar Food Industry and Business Company	-	1.97
Sodium hydroxide (>97%)	NaOH	Activating agent	Merck Milipore	39.997	2.13
Sulfuric acid (95%)	H_2SO_4	Precipitating agent	Merck Milipore	98.079	1.84
Ethanol (>96%)	C_2H_5OH	Washing solvent	Merck Milipore	46.07	0.79 (20^OC)
3-aminopropyl triethoysilane	$H_2N(CH_2)_3Si(OC_2H_5)_3$ (APTES)	Functionalizing agent	Momentive	221.372	0.95 (25^OC)

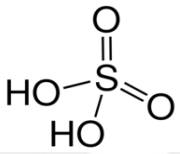

(a) Sulfuric acid

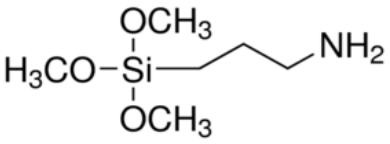

(b) Aptes

Figure 2.1 The chemical structure of sulfuric acid and APTES used.

2.2 Characterization of Gels and Particles

The characterization methods performed during experiments, equipments' brands/models and the purpose of using these analysis methods are given in Table 2.2.

Table 2.2 Analysis methods used during experiments.

Equipment	Brand/Model	Purpose of use
Atomic Absorption Spectrophotometer (AAS)	Agilent Duo 240240F_s/240F_s Ultra	Determination of ion concentration in liquids
Brunauer-Emmett-Teller (BET) Analysis Device	ASAP 2010 Micrometrics	Determination of surface area and porosity of the materials.
Dynamic Light Scattering Device (DLS)	Malvern Zeta-nanosizer S90 equipped with He-Ne laser	Determination of zeta potentials and size of the materials
Fourier Transform Infrared Spectrophotometer (FT-IR)	Thermo Scientific Nicolet iS5, iD1 Transmission (ATR Apparatus), Scan number: 32, Resolution: 4	Determination of the characteristic bonds and organic groups
Inductively Coupled Plasma Mass Spectrometer (ICP-MS)	Agilent 7500e	Determination of elements of particles
Scanning Electron Microscope (SEM)	Philips XL-30S FEG	Determination of shape and size of the particles' surface
Transmission Electron Microscope (TEM)	TEM-MSC JEOL 2100	Determination of inner structure of the particle
Thermogravimetric Analysis Device (TGA)	TA Q500	Analyzing of the weight change of materials
UV-Visible Spectrophotometer (UV-Vis)	UV-2600 20V EN, 50-60 Hz, 170 VA, Shimadzu	Evaluation of the drug concentration in the liquid phase
X-Ray Diffractometer (XRD)	Philips X-pert PRO-45W, 40 mA using λ=0.1541, 2θ between 5 and 80°	Determination of the characteristic bonds
X-Ray Photoelectron Spectroscopy Device (XPS)	Thermo Nexsa XPS	Determination of the chemical bonds of the atoms on the solid surface

2.2.1 Atomic Absorption Spectrophotometer

Atomic absorption spectrophotometry is an analytical technique that determines the concentrations of elements. The brand/model of AAS used in the experiment is given in Table 2.2. The calibration curves for Na^+ and Si^{4+} ions are listed in Figure 2.2 and Figure 2.3, respectively. Figure 2.4 represents the image of AAS device used. For both ions, acetylene was used as fuel in the experiments. Lamp current is fixed as 5 mA and 10 mA, support is air and nitrous oxide for Na and Si ion. For Na^+ ion, the wavelength and slid width worked in atomic absorption is 330.2 nm and 0.5 nm, respectively. For Si^{4+} ion, the wavelength and slid width worked in atomic absorption is 251.6 nm and 0.2 nm, respectively.

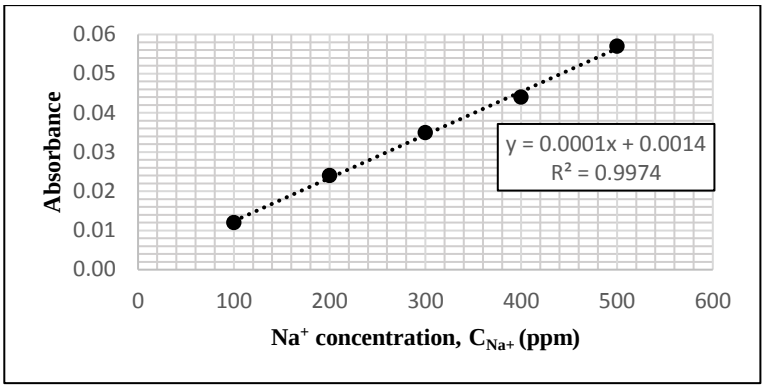

Figure 2.2 Calibration curve of standard solutions for Na^{+}ion at 25°C.

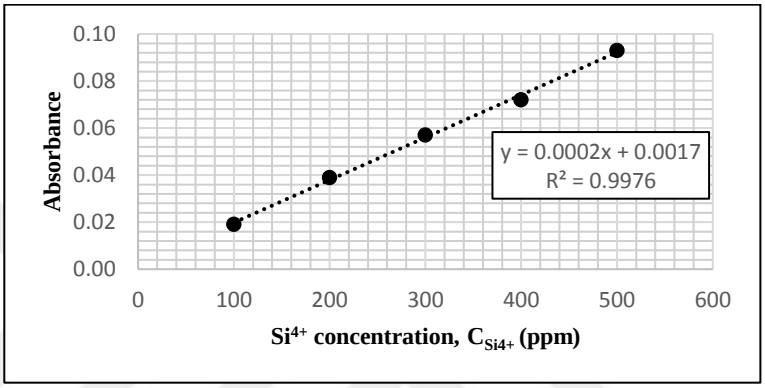

Figure 2.3 Calibration curve of standard solutions for Si^{4+}ion at 25°C.

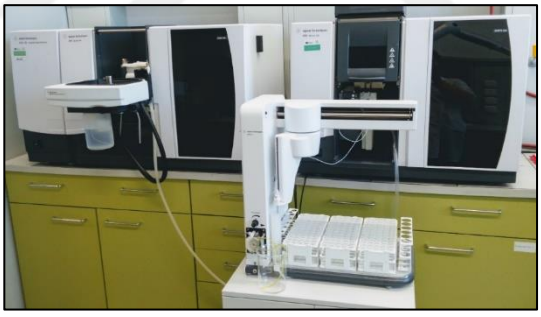

Figure 2.4 Photograph of AAS device used.

2.2.2 Surface Area and Porosity

BET Analysis device is able to detect surface area measurements such as micro, meso and macro pore size.

Baret-Joyner-Halenda analysis uses adsorption/desorption techniques and can measure specific surface area and pore volume. This analysis gives pore size distribution independent of external area due to particle size.

The image of BET analysis device used is shown in Figure 2.5.

Figure 2.5 Photograph of BET analysis device used.

2.2.3 Dynamic Light Scattering

DLS device uses electrophoretic light scattering technology to measure zeta potential. The speed of movement in the dispesion of a solution or particles by creating an electrical field is the zeta potential. Figure 2.6 shows the image of the DLS device used.

DLS device also determines Brownian motion and relates this to the size of the particles by assuming that the samples contains of spherical particles. Brownian motion is the random movement of particles due to the bombardment by the solvent molecules that surround them. It should be noted that the diameter that is obtained in DLS shows how a particle diffuses within a fluid so it is calledas a hydrodynamic diameter.

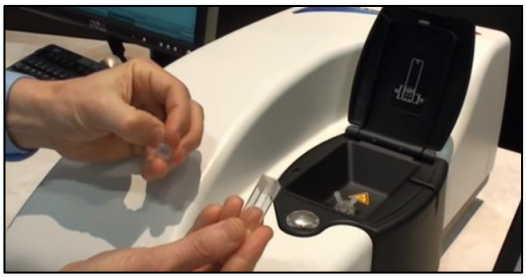

Figure 2.6 Photograph of DLS device used.

A collection of objects is called monodisperse if the objects have the same size, shape or mass. A sample of objects that have an inconsistent size, shape and mass distribution is called polydisperse. The PDI is an indication of variance in the

sample, a low PDI (usually less than 0.2) indicates that the sample is monodispersed.

The procedure for size and zeta potential measurement is as follows: 27 mg of S/S-APTES nano particles are dissolved in 30 ml of double distilled water and stirred for 3 hours. Immediately after stopping stirring, the sample is taken from the middle of the solution and the size measurement is performed for once. Amount of run is adjusted to 6 and the cuvette, solvent and particle type is chosen in the settings. If the particle type is not present in the list, refractive index of the particle should be found in the literature and added to the list. The solutions are kept without stirring for 24 hours in the room temperature. During this time, electrostatic attraction/repulsion balance between particles is achieved and then, zeta potential of the particles are measured.

2.2.4 Fourier Transform-Infrared Spectrophotometer

The functional groups in the structure of organic compounds in any phase. Also amino acids and proteins's structure biochemically. Figure 2.7 gives the image of the FT-IR device that was used in the study.

Figure 2.7 Photograph of FT-IR device used.

2.2.5 Inductive Coupled Plasma Mass Spectrophotometer

ICP-MS is an analysis technique that allows the accurate measurement of a large number of elements in solid and liquid samples. With ICP-

MS technology, 77 elements can be analyzed simultaneously solid/liquid particles. Analysis of up to 35 elements in a single sample by ICP-MS can be determined in a few minutes.

The procedure for ICP-MS measurement is as follows: The grinded rice husk ash (0.2 g), the lithium tetra borate (1 g) and lithium meta borate (1 g) were mixed and put into the platinum crucible. This mixture was calcined in the preheated muffle furnace at 1000^{o}C for 1h. After calcination process the entire base of the platinum crucible is quickly rinsed with cool double distilled water so that the transparent solid in the crucible is broken. Then the magnetic bar is placed in the crucible and the crucible is put in the beaker which was filled with 125 ml of nitric acid in weight percentage of 5. At the end of the mixing the crucible is thoroughly washed and separated from this solution. The resulting solution is poured into a 250 ml volumetric flask and it is filled with double distilled water until the volume is 250 ml. This final solution is kept in the cold medium and the elemental analysis is performed in ICP-MS instrument (Figure 2.8).

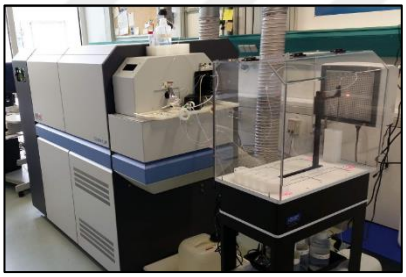

Figure 2.8 Photograph of ICP-MS device used.

2.2.6 Transmission Electron Microscope

Transmission electron microscope is a microscopic device. The main difference between SEM and TEM is that SEM creates an image by detecting reflected electrons while TEM uses transmitted electrons to create an image. Obtained information from TEM is more valuable about inner structure whereas SEM gives information on the sample's surface and its composition (Manual of Thermo Fischer's TEM, Figure 2.9).

Figure 2.9 Photograph of TEM device used.

TEM measurements were performed in the laboratories of Centre of Polymer Systems in Tomas Bata University in Zlín in Czech Republic.

2.2.7 Thermal Gravimetric Analyzer

Thermal gravimetric analyzer is generally used to determine mass loss in materials as a function of temperature/time. In the analysis performed in this study, temperature was chosen as the function parameter. The test sample is heated at a constant heating rate (10 °C/min) and the mass change of the sample is measured and recorded as a function of temperature (room temperature to 1000 °C). In general, reactions that cause the mass of the sample can be either degradation/oxidation reaction or evaporation of a component.

Figure 2.10 Photograph of TGA device used.

2.2.8 Ultra-Violet Visible Spectrophotometer

The ultraviolet-visible (UV-Vis) spectrophotometer is an instrument commonly used in the laboratory that analyzes compounds in the ultraviolet (UV)

and visible (Vis) regions of the electromagnetic spectrum. Unlike infrared spectroscopy (which looks at vibrational motions), ultraviolet-visible spectroscopy analyze the electronic transitions. It allows one to determine the wavelength and maximum absorbance of compounds. From the absorbance information and using a relationship known as Beer's Law one is able to determine either the concentration of a sample if the molar extinction coefficient is known, or the molar absorptivity, if the concentration is known:

$$A=\varepsilon bc \qquad \text{(Miller et al., 2009)}$$

where A is absorbance, ε molar extinction coefficient, b path length, and c concentration.

The drug concentration of CFD in the liquid phase was determined by UV-Vis spectrophotometer at its characteristics wavelength of 272 nm. The calibration curves for CFD in double distilled water (DDW) at pH=1.2 and pH=2 are given in Figure 2.11 and Figure 2.12, respectively.

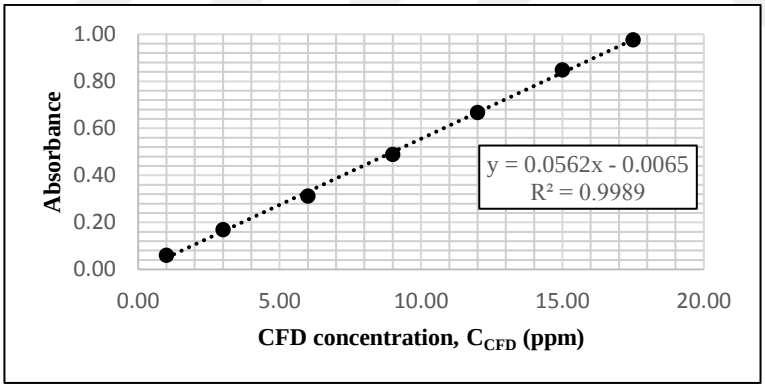

Figure 2.11 Calibration curve of standard solutions for CFD in DDW at pH 1.2.

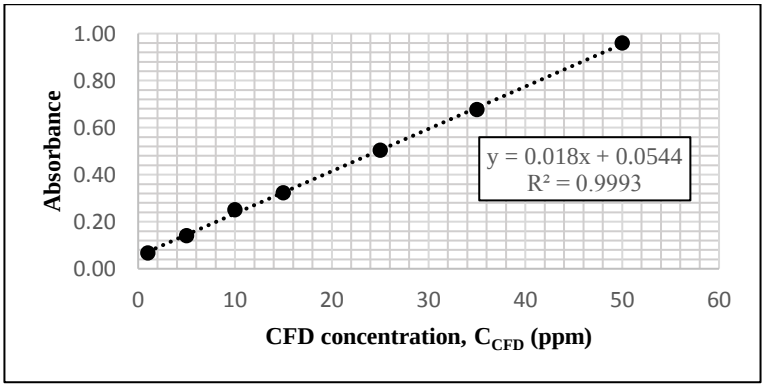

Figure 2.12 Calibration curve of standard solutions for CFD in DDW at pH 2.

Figure 2.13 Photograph of UV-Vis device used.

2.2.9 X-Ray Photoelectron Spectrophotometer

X-ray photoelectron spectroscopy is a quantitative spectroscopic technique that measures the elemental composition, empirical formula, chemical state and electronic state of the elements that exist within a material (Figure 2.14).

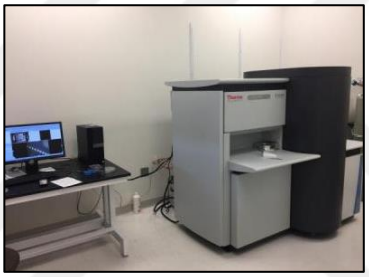

Figure 2.14 Photograph of XPS device used.

2.2.10 X-Ray Diffractometer

XRD analysis investigates crystalline material structure, including atomic arrangement, crystalline size and imperfections. It is a non-destructive technique for analyzing a wide range of materials including metals, minerals, polymers, catalysts, plastics and pharmaceuticals. The done analysis is spot scanning and the number of the scanning is 3. X-ray light source is Al Kα monochromatic (1486.68 eV) and X-ray point dimension is 300 μm. The analyzer is 180 ° semispherical type analyzer which has a sensor with 128 channels and it works with an energy of 30 eV. Figure 2.15 displays the image of XRD device.

Figure 2.15 Photograph of XRD device used.

2.3 Methods

2.3.1 Synthesis of silica alcogel from rice husk ash (S)

The pathway followed for the production of silica alcogel from rice husk ash is represented figuratively in Figure 2.18. Particle synthesis is performed by physicochemical method involving two steps: alkali dissolution with precursor rice husk ash and acidic precipitation with sulfuric acid (Thuadaji and Nuntija, 2008).

20 grams of milled rice husk ash approximately in the size of 0.2 mm are mixed with the 160 mL of NaOH solution in molar ratio of 2.5 N at 550 rpm in 500 mL reactor for 30 min and then boiled under reflux at 120^{o}C for 3 h at mixing speed of 450 rpm. At the end of the reaction period two phases are formed. One of them is undissolved black solid impurities settled at the bottom of the reactor and the other is supernatant above it. The solid impurities settled and the supernatant are separated from each other for further treatments. Later precipitation is carried out by adding sulfuric acid in molar ratio of 5 N into the supernatant (sodium silicate solution) in 2 h until the pH of the solution becomes neutral. At the end of the precipitation two phases are formed. White precipitate is silica gel. After separating these two phases, the silica gel is aged for 3 h at room temperature and then washed for several times with boiling double distilled water to remove Na^{+} ions. Rinsing of the silica gel was repeated until pH of the washing waters become neutral. The white neutral silica gel is called as hydrogel. The hydrogel is mixed with ethanol for 8 h at 80°C to change solvent from water to organic phase and dried at 110 °C for 24 h. During the rinsing process and the solvent change, the stirring duration was fixed as 30 min.

The efficiency of sodium silicate and extraction were controlled with AAS technique. The images of the extraction process and the filtration step are shown in Figure 2.6 and 2.17.

Figure 2.16 The extraction process.

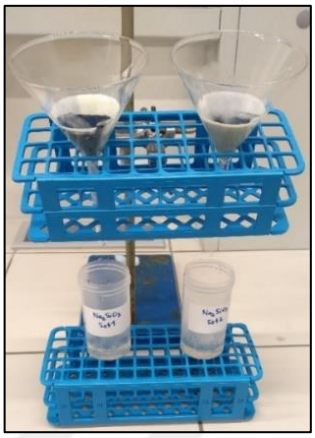

Figure 2.17 The filtration step.

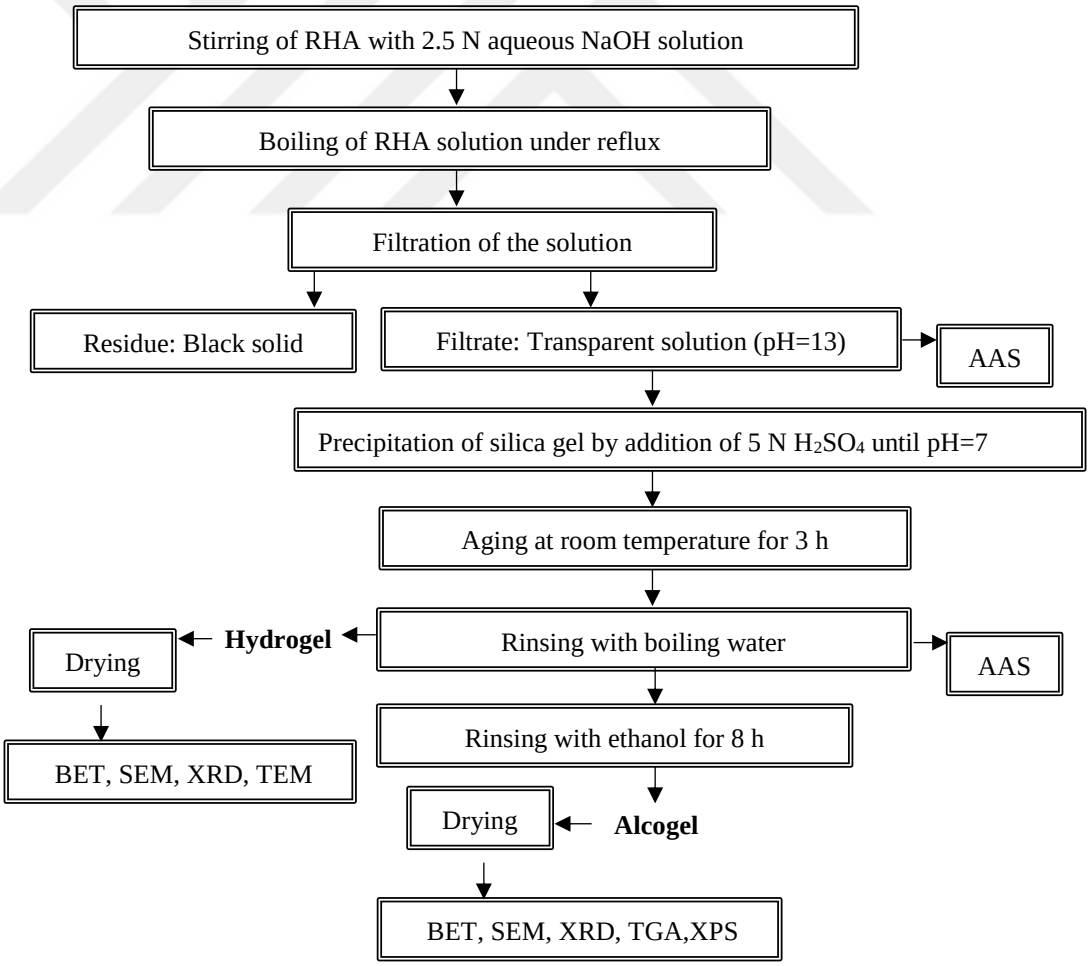

Figure 2.18 Schematic representation of extraction of silica from RHA by TH method.

2.3.2 Functionalization of silica alcogel surfaces by APTES (S-APTES)

Post-grafting method was used for functionalization of silica alcogel. Ethanol and APTES were chosen as reaction medium and functionalization agent, respectively. Experiments were carried out in jacketed glass reactors and spiral condensers were used to avoid evaporation of reaction medium. Effect of temperature and silane/SiO_2 molar ratio were investigated (Table 2.3). These parameters were determined after literature survey. In the literature, the most studied temperatures are 25, 40 and 70°C (Table 1.5) and the most studied molar ratio of APTES/SiO_2 is between 0.2 and 0.6.

Firstly silane and silica alcogel were dispersed in separate 30 ml of ethanol solutions and mixed well for 30 min (Appendix). After obtaining well dispersed suspensions, silane dispersed mixture and 70 mL of ethanol is added into silica alcogel dispersed mixture and the final mixture was refluxed for 24 h to achieve functionalization at varying temperatures. After functionalization, the suspension is centrifuged at 6000 rpm for 5 min and washed with ethanol twice. The resulting precipitates (S-APTES) are vacuumed dried overnight at 110 °C. The experimental conditions are given in Table 2.3.

Table 2.3 Experimental conditions of post functionalization method.

Experiment no.	T (°C)	n_{Aptes}/n_{SiO2}	V_{EtOH} (ml)	V_{Aptes} (ml)
1	25	0.2	130	2.34
2	25	0.4	130	4.68
3	25	0.6	130	7.02
4	50	0.2	130	2.34
5	50	0.4	130	4.68
6	50	0.6	130	7.02
7	70	0.2	130	2.34
8	70	0.4	130	4.68
9	70	0.6	130	7.02

2.3.3 Loading of cefdinir

For a good loading, the surface charge of the drug and particle should be different and in this study it presents only at pH 2. So pH 2 was chosen as loading medium after determining the zeta potentials of CFD, S and S-APTES nanoparticles at pH 2, 4, 6, 8 and 10. CFD has the highest solubility at pH 8 (Cho et al., 2017) so it is dissolved in double distilled water at pH 8 for 24 h. The pH of the CFD solution was adjusted to pH 2 by addition of 0.1 N HCl. For all loading studies, CFD solution at pH 2 was used. Experiments were carried out in jacketed glass reactors and spiral

condensers were used to avoid evaporation of reaction medium. The stirring rate was kept as 450 rpm.

During the CFD loading process, different amount of silica nanoparticles was weighed and 276 ppm CFD solution was prepared (This is the maximum concentration amount of CFD which could be dissolved in double distilled water). The particles were poured into 30 ml of CFD solution and stirred for 40 h at 37°C. CFD loading procedure was performed by using four different amount of S and S-APTES nanoparticles (C_{CFD}/C_S) to control whether the amount influences drug loading or not. These concentration amounts were listed in Table 2.4 and 2.5 below.

Table 2.4 The list of the amount of S nanoparticles.

C_{CFD} (ppm)	m_S (mg)	C_{CFD} / C_S
276	13.5	0.61
276	27	0.31
276	54	0.15
276	108	0.08

Table 2.5 The list of the amount of S-APTES nanoparticles.

C_{CFD} (ppm)	$m_{S\text{-}APTES}$ (mg)	C_{CFD} / C_S
276	27	0.31
276	54	0.15
276	108	0.08
276	216	0.04

2.3.4 In-vitro cefdinir release

The in-vitro CFD diffusion from the pure and functionalized silica alcogel nanoparticles is examined by dialysis membrane (Membra-cell MD34, MWDO: 14000 Da) to separate the dissolution and nanoparticle suspension medium. The dissolution medium used is 0.1 M HCl solution (pH 1.2). The 10 mg/10 ml of CFD loaded pure and functionalized silica nanoparticle suspension was immerged into dialysis membrane in 200 ml HCl solution. The temperature was kept at 37°C in order to stimulate the temperature of the human body. The dissolution medium was stirred at speed of 450 rpm using magnetic stirrer. As time increases, 1 ml were taken out from the dissolution medium at predetermined time intervals and UV-Vis was used to quantify the amount of CFD released. Figure 2.19 represents the image of release experiment.

Figure 2.19 Experimental set-up for release experiment.

3. RESULTS AND DISCUSSION

3.1 Determination of the Content of Rice Husk Ash

The contents of rice husk ash used for silica production are determined by ICP-MS as described in Section 2.2.5. The results obtained from ICP-MS characterization are given in Table 3.1.

Table 3.1 Composition of rice husk ash.

Elements	Rice husk ash (%)
SiO_2	52.83
Al_2O_3	0.1
Fe_2O_3	0.03
CaO	0.8
MgO	0.25
Na_2O	0.24
K_2O	3.26
TiO_2	0
MnO	0.17
C	42.32

ICP-MS analysis indicated that rice husk ash consists of small amounts of elements such as Al, Fe, Ca, Mg, Na, K, Ti. It can also be seen from this table that rice husk ash contains high amount of silicon and carbon element as expected from the literature.

3.2 Size Distribution of Silica Particles

Seven sodium silicate solutions (SSS) were produced to see the reproducubility. The size distributions of silica in SSSs are given in Figure 3.1 in terms of intensity. As it can be seen from Figure 3.1, SSSs are reproducible since all the dispersions gave peaks in the same range. The first of these peaks is located at around 2-3 nm in size, and the second peak is mostly around 100-400 nm and the third peak is seen around the range of 1500-5000 nm (Figure 3.1). The dispersions were directly measured without being dissolved in a solvent.

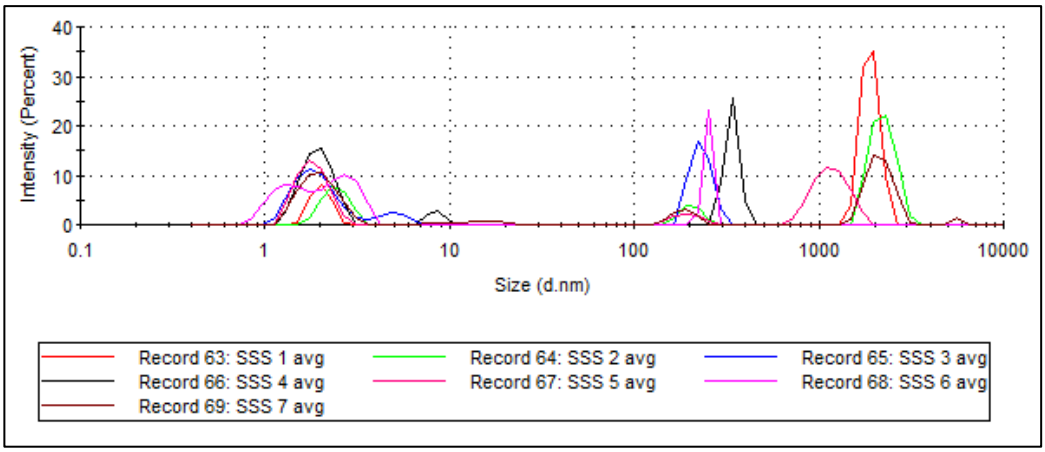

Figure 3.1 Size distribution by intensity of the SSSs.

The results of DLS measurements are tabulated in Table 3.2. It can be observed from Table 3.2 that the majority of the particle size distributions consist of 2-3 nm. PDI values varies between 0.2 and 1 which means that the silica particles in the SSSs were agglomerated.

Table 3.2 Results of DLS measurements.

Sample	PDI	Peak 1			Peak 2			Peak 3		
		d_{mean} (nm)	Int. (%)	St. Dev. (nm)	d_{mean} (nm)	Int. (%)	St. Dev. (nm)	d_{mean} (nm)	Int. (%)	St. Dev. (nm)
SSS 1	0.46	2.0	19.3	0.24	-	-	-	1895	80.7	211.7
SSS 2	0.44	2.4	23.5	0.38	-	-	-	2219	76.5	337.6
SSS 3	0.93	1.9	57.7	0.51	230.0	42.3	29.8	-	-	-
SSS 4	1.00	1.9	61.3	0.36	338.7	38.7	28.7	-	-	-
SSS 5	0.96	1.8	53.2	0.35	-	-	-	1170	46.8	245.7
SSS 6	0.78	2.5	42.9	0.57	251.7	24.2	10.2	-	-	-
SSS 7	0.25	2.0	44.2	0.44	-	-	-	2130	50.9	329.7

3.3 Effect of Solvent Change on Surface Properties of Hydro and Alcogels

It can be seen from the Table 3.3 that S and S-APTES particles are reproducible because the surface area and the pore diameter values gives very close values. In drug loading, the particle must be enough large to intake the drug. In this study, pore diameters of hydrogels is around 6.2 nm which is a good value because diameter of a CFD molecule is 2.2 nm. If ethanol is used as solvent, pore diameter decreases however surface area increases around 50 m^2/g averagely in case of solvent change. Surface area is also quite important parameter in drug loading.

Table 3.3 BET Analysis results of hydrogel and alcogel.

Solvent type	Sample	BET surface area (m^2/g)[a]	External surface area (m^2/g)[b]	d_{pore} (nm)[c]
Boiling water	1	190.3	183.1	6.1
	2	208.7	199.4	6.3
	3	194.9	186.5	6.2
EtOH	1	248.2	228.4	5.9
	2	244.8	230.8	6.1
	3	145.0	136.0	5.4

[a]: BET surface area was derived from adsorption data.

[b]: External surface area was derived from t plots.

[c]: Mesopore average diameter was derived using BJH method.

3.4 X-Ray Diffraction Pattern of S and S-APTES Particles

Figure 3.2 indicates the XRD patterns of pure and functionalized silica powders. Amorphous silica was confirmed with the broad peak at 25-30° (Chen et al., 2017; Ghorbani et al., 2015). There is no significant change in XRD spectrums of particles functionalized at different conditions. All peaks could not be observed clearly due to instrumental limitations.

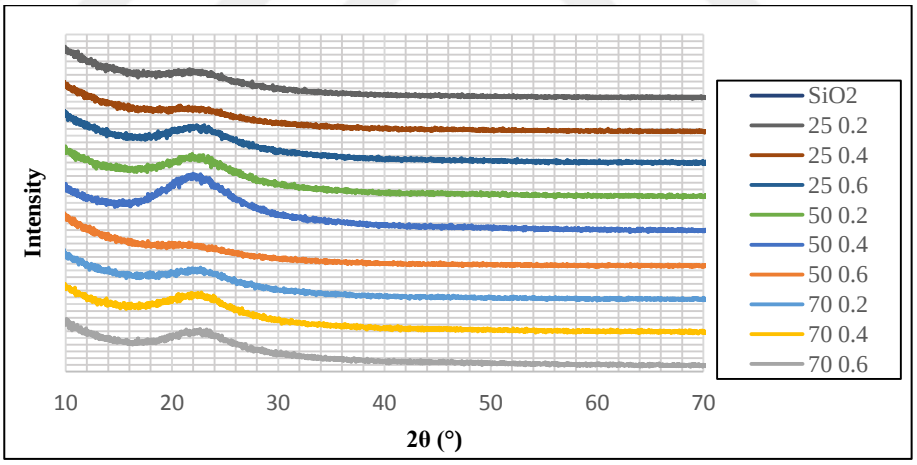

Figure 3.2 XRD patterns of S and APTES modified nanoparticles.

3.5 FT-IR Spectra of S Particles

The FT-IR spectra of pure silica sample produced is given in Figure 3.3. There is a small band in 3000-3500 cm^{-1} referring to the stretching vibrations of silanol groups (Si-OH) and a small peak at 1639 cm^{-1} which refers to bending vibrations of silanol groups. There is a very strong peak at 1082 cm^{-1} due to asymmetric Si-O-Si

stretching and a smaller peak at 790 cm^{-1} belonging to the symmetric vibrations of the Si-O-Si stretching. Silica formation was approved by these characteristic bands and supported by the literature researches (Liou and Lin, 2012; Sankar et al., 2016).

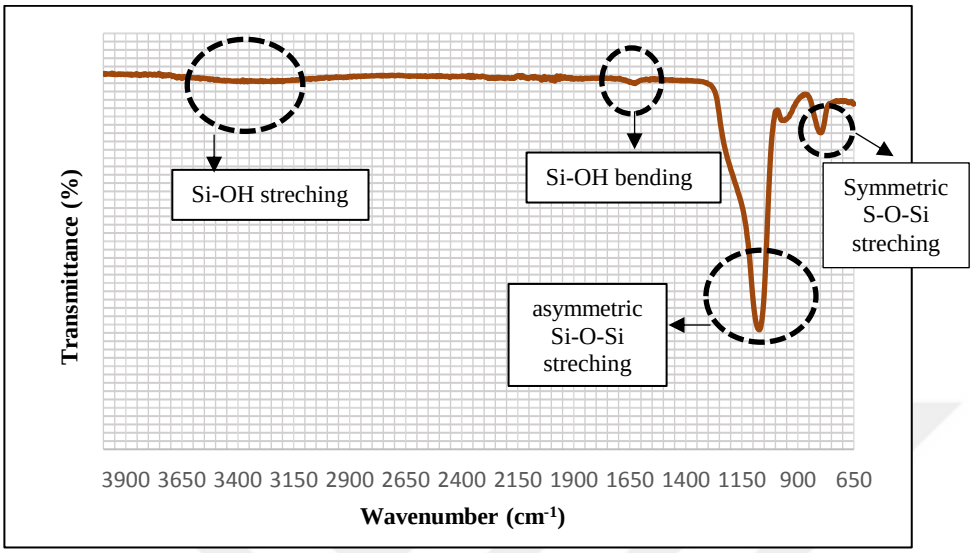

Figure 3.3 FT-IR spectra of S nanoparticles.

3.6 Thermal Analysis of S and S-APTES Particles

The thermogravimetric analysis was performed to investigate the amount of grafted APTES. For comparison purposes also unmodified hydrogel and alcogel samples were exposed to thermal analysis. For functionalization, the highest mass loss shows the highest coverage. It can be seen from the Figure 3.4 that the mass loss in the temperature ranges 25-150 °C about 12.96% for alcogel and 9 % for hydrogel. This loss is attributed to desorption of water in the pores and H-bonded to silanol groups of silica surface. Additonally, there is a rapid decrease in the range of 200-650 °C that belongs to the the decomposition of organic functionalities which was also confirmed by literature research of the post modification of silica (Malhis et. al., 2017).

Figure 3.4 show that there is a direct relation between molar ratio and the mass loss. Except one point, as the molar ratio increases at each temperature, the mass loss increases. The point which does not obey these tendency: (50°C, n_{Aptes}/n_{SiO2}=1.2). It means that after a certain amount of APTES, the molecular

interactions between APTES molecules is so high that the functionalization efficiency decreases. The mass increases from 25°C to 50°C but at 70°C the mass loss decrease. The maximum mass losses were seen at 50°C (Table 3.4). The biggest amount of mass loss occurred at 50°C for the ratio n_{Aptes}/n_{SiO2}=0.6. This was the optimum condition for functionalization. Table 3.4 shows the mass losses at each point.

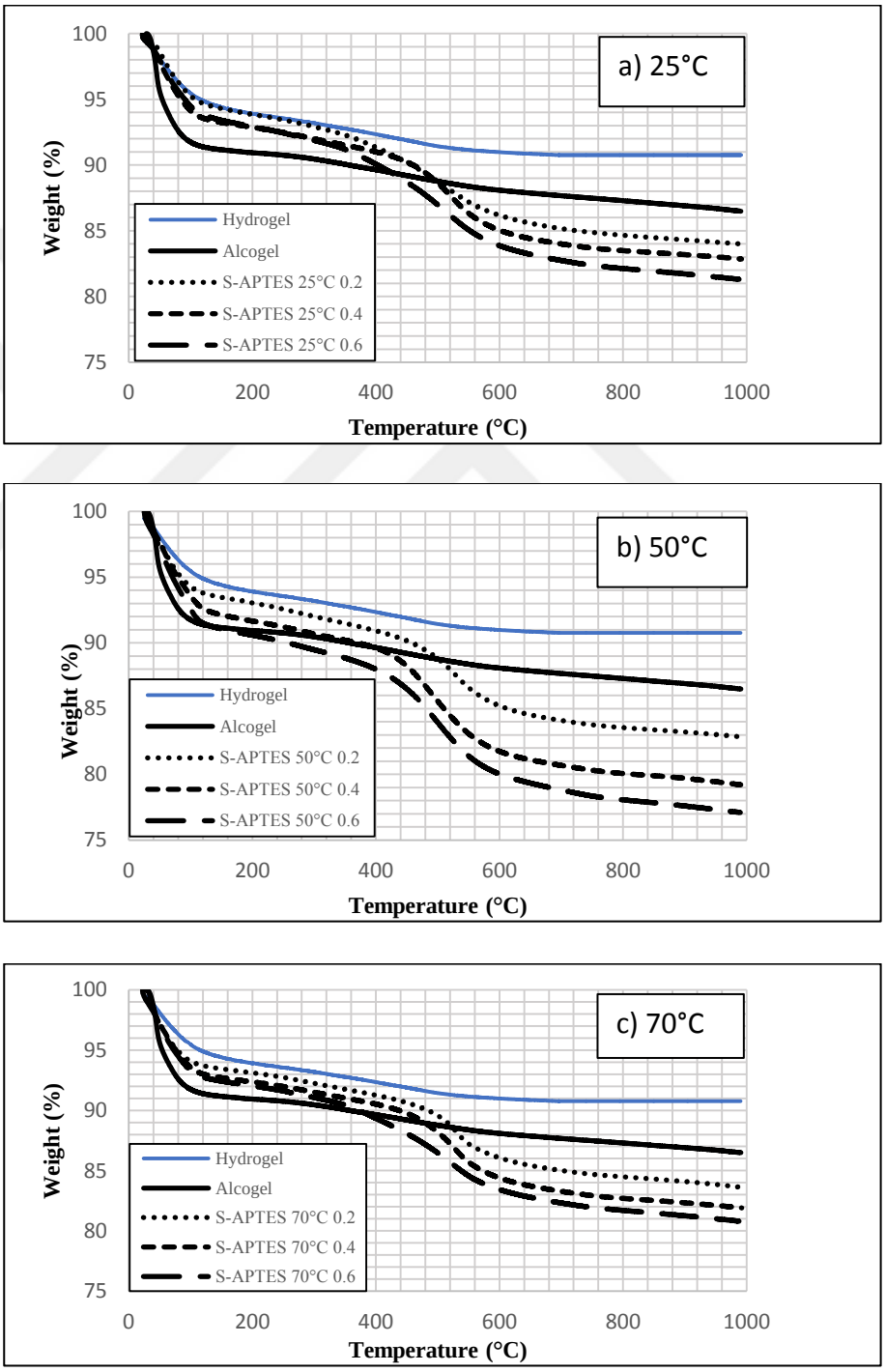

Figure 3.4 TGA thermograms of S and S-APTES nps modified at 25°C(a), 50°C (b) and 70°C (c).

Table 3.4 The mass losses at TGA thermograms.

Sample	**The mass loss (%)**
Hydrogel	9.00
Alcogel	12.96
S-Aptes at 25°C 0.2	15.99
S-Aptes at 25°C 0.4	17.15
S-Aptes at 25°C 0.6	18.68
S-Aptes at 50°C 0.2	17.16
S-Aptes at 50°C 0.4	20.81
S-Aptes at 50°C 0.6	22.91
S-Aptes at 50°C 1.2	21.38
S-Aptes at 70°C 0.2	16.39
S-Aptes at 70°C 0.4	18.09
S-Aptes at 70°C 0.6	19.22

3.7 Characterization of S and S-APTES Particles using XPS Analysis

The chemical state of the pure silica and the samples which shown the highest two mass loss in TGA results (n_{Aptes}/n_{SiO2}=0.6 and 1.2) after APTES functionalization were examined by high resolution XPS measurements which was represented in Figure 3.5 and 3.7. The wide XPS scan displays signals due to carbon, oxygen, silicon, nitrogen and sodium. Figure 3.6 shows the enlarged regions of XPS spectra of S particles. The prominent peaks for Si 2p, O 1s, C 1s and N 1s are consistent with the formation of silica nanoparticles bearing hydrolyzed APTES molecules on their surface. The Si 2p spectra (Figure 3.6a) consists of a distinct peak centered at 102.98 eV, characteristic of Si-O bonds. The C 1s peaks peak (Figure 3.6b) centered at 284.58 eV supports the existence of the C-C bonds of the hydrolyzed APTES molecules. The N 1s spectra at 399.28 eV (Figure 3.6c) confirms the presence of primary amine N-H bonds (Chandra et al., 2017). 532.38 eV (Figure 3.6d) shows the presence of O and finally Na 1s spectra at 1072.08 eV (Figure 3.6e) proves the presence of Na atoms, which means that the Na ions could be removed from the hydrogel very well in washing step after precipitation of sodium silicate solution however the percentages of Na atom (Table 3.5) is very low which shows there is a trace amount of Na inside of the alcogel. It can be also conclude from Table 3.9 and 3.10 that as the ratio of silane increases presence of N atoms increase and the atom O increased by increasing the ratio from 0.6 to 1.2.

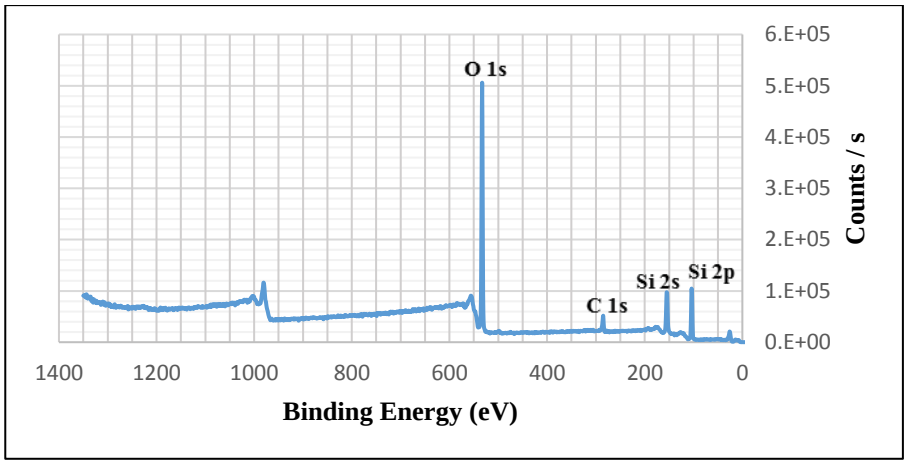

Figure 3.5 The wide scan XPS spectra of the S nanoparticles.

Table 3.5 Atomic composition of S nps.

Element	Atomic content (%)		
	Pure silica	n_{Aptes}/n_{SiO2}= 0.6	n_{Aptes}/n_{SiO2}= 1.2
Si	31.92	26.38	26.14
C	10.63	24.79	19.36
N	-	4.96	5.83
O	56.23	42.79	45.03
Na	1.22	1.08	-

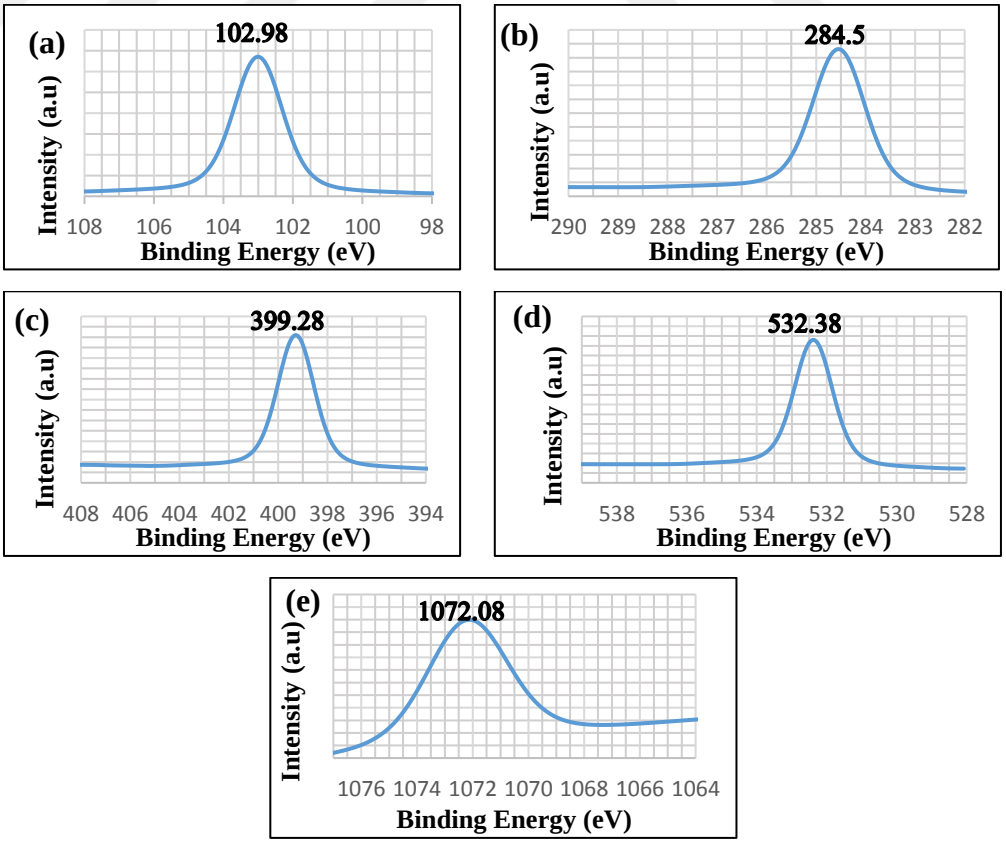

Figure 3.6 The enlarged regions of XPS spectra of Si2p(a), C1s (b), N1s (c), O1s (d) and Na1s (e).

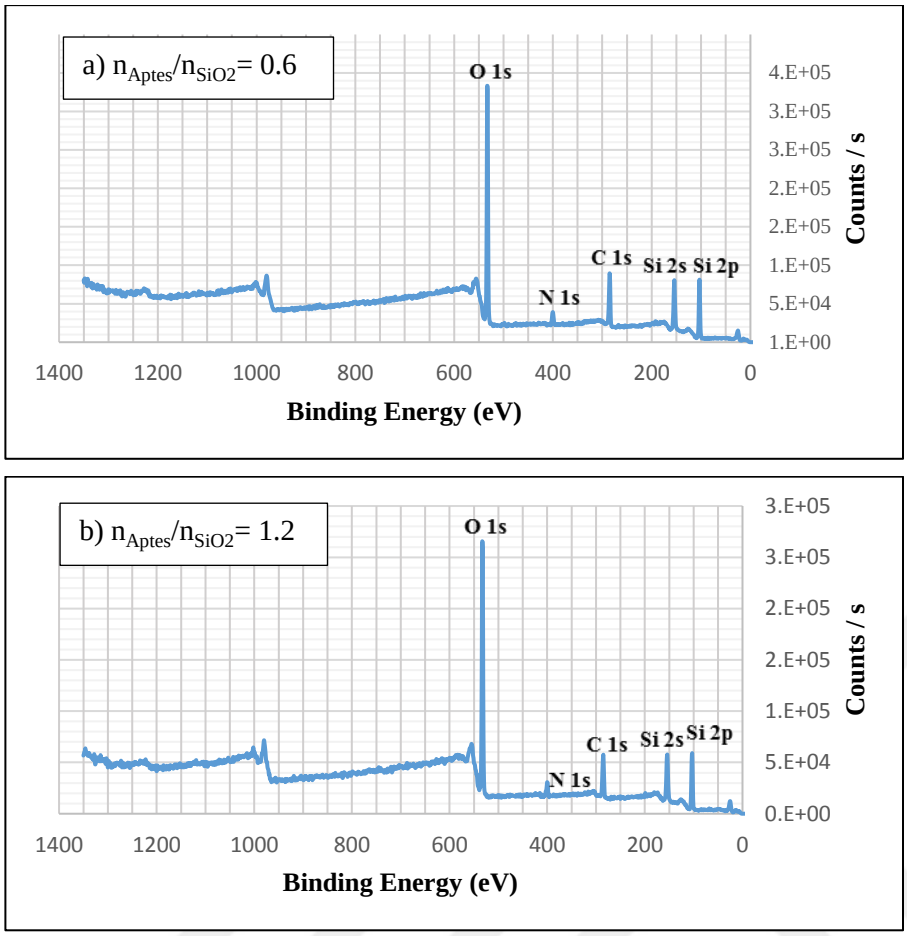

Figure 3.7 The wide scan XPS spectra of the S-APTES nanoparticles functionalized at n_{Aptes}/n_{SiO2}= 0.6 (a) and n_{Aptes}/n_{SiO2}= 1.2 (b).

When we compare the ratios 0.6 ad 1.2, it is thought that the reason for biggest mass loss at n_{Aptes}/n_{SiO2}=0.6 in TGA analysis is the bulky attached APTES molecules onto these S-APTES particles. Thanks to XPS that, this method proves the chemical bonds in the molecules and fixed this complexity.

As a result n_{Aptes}/n_{SiO2}=1.2 was the best ratio among the all parameters. Please note that, here in this study n_{Aptes}/n_{SiO2}= 0.6 was used as the chosen S-APTES since the time was limited to produce S-APTES particles enough at n_{Aptes}/n_{SiO2}= 1.2.

3.8 Particle Morphology of Hydrogel, Alcogel and S-APTES

The SEM images of hydrogel, alcogel and best S-APTES nanoparticles were given in Figure 3.8. All of the particles have irregular shapes. Hydrogel looks like a cloud and there is no shape of it. The silica particles in hydrogel are apparently

agglomerated and size cannot be measured. Alcogel particles also agglomerated however the agglomeration clusters' surface looks harder and like having more certain borders with each other. Lastly it can be seen from the Figure 3.8 that the grains begin to disintegrate.

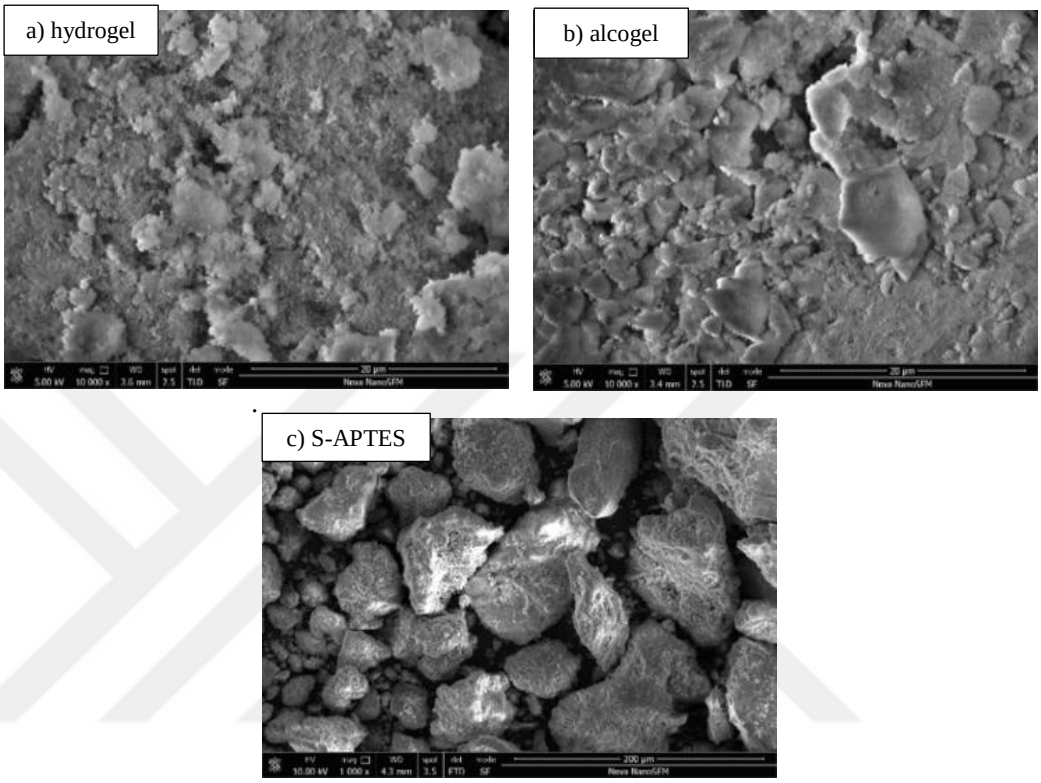

Figure 3.8 SEM micrograph of hydrogel (a), alcogel (b) and S-APTES with the ratio of 0.6.

3.9 Characterization of S and S-APTES Particles using TEM

TEM images of dried alcogel and best S-APTES powder are given in Figure 3.9. It can be easily seen from the figure that the particle diameter decreased after functionalization. Before functionalization, the diameter of the particles was between 5-20 nm whereas the diameter after functionalization was around 10 nm. In both cases the particles agglomerated but it seems that the functionalization made the pure silica nanoparticles to have a more uniform distribution.

The particle sizes in TEM images are smaller than that of SEM images. The reason of this is that acetone was used to disperse the powders before taking TEM images and this helped to have a better image by TEM. On the contrary in analysis of SEM, solutions were directly used without any dispersion in any solvent.

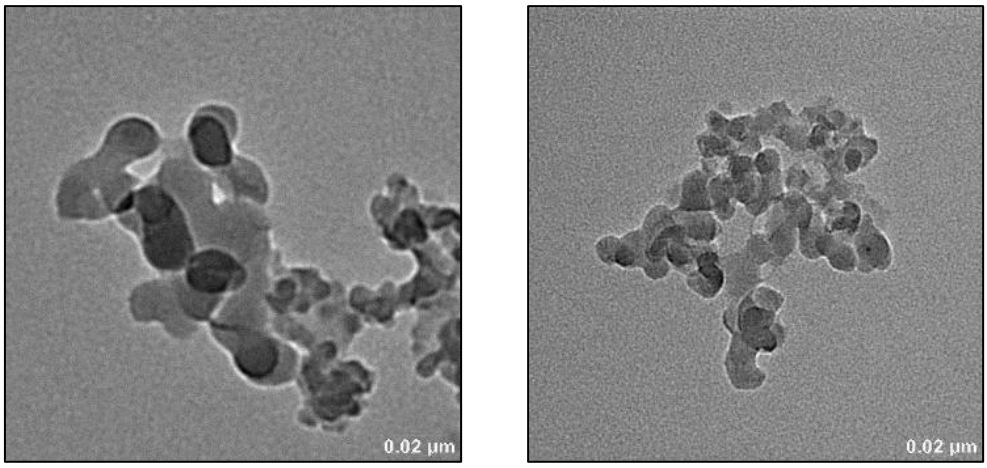

Figure 3.9 TEM images of S and S-APTES nanoparticles.

3.10 Zeta potential measurements of CFD, S and S-APTES particles

The zeta potential of S, S-APTES and CFD are given in Figure 3.10. From the Figure 3.10 it can be seen that the surface charge of CFD is always negative in all pH values however the particles have isoelectronic points. Isoelectric points are the points where the surface charge is zero and there is no attraction/repulsion between particles. The isoelectric points of S and S-APTES are approximately 3 and 4, resectively. The most appropriate pH value for loading is pH 2 since the surface charge of the drug and particles are different.

From the zeta potential charts, the stability can be read. If the zeta potential of the particle is between -30 and 30, the dispersion is unstable however if this value is out of this range, the dispersion is stable. Figure 3.10 shows that CFD is unstable in all pH values, S-APTES dispersion is stable at only pH 2 and S is stable at pH values above 3.5.

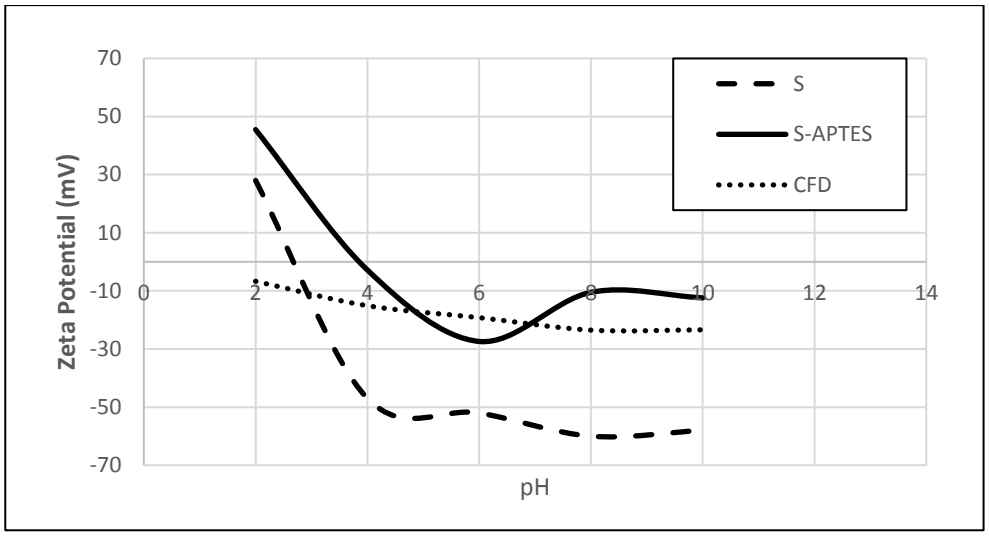

Figure 3.10 Zeta potential of S, S-APTES and CFD at different pH values 2, 4, 6, 8 and 10.

3.11 Loading of cefdinir

Different amounts of adsorbents (S and S-APTES) were studied in the drug loading part. Concentration of CFD solution was fixed as 276 ppm. All loading experiments were studied three times to see the repeatability. Average loading percentages are plotted in Figure 3.11.

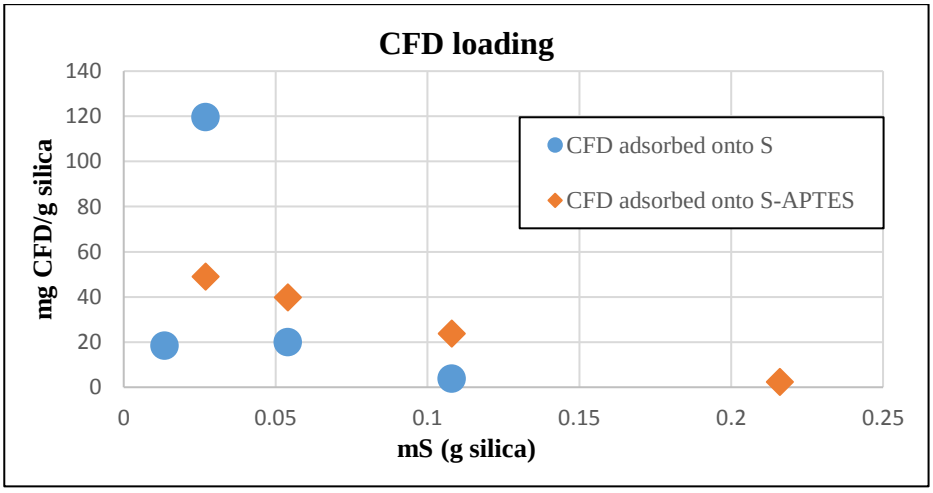

Figure 3.11 CFD loading onto S and S-APTES nanoparticles at 25°C.

Loading process was more successful in S particles compared to S-APTES particles. 39% of CFD could be loaded into S particles however only 31% of CFD could be loaded into S-APTES particles. For the pure silica samples, the best

loading was achieved with the ratio C_{CFD}/C_S=0.31. As the amount of drug carrier increased, the loading percentage increased for loading of CFD into S particles. For the S-APTES particles instead, a better loading was succeeded as the amount of drug carrier decreased. The most appropriate loading was seen at the ratio $C_{CFD}/C_{S\text{-}Aptes}$=0.08.

3.12 Release Experiments and Kinetic Models

Among the pure silica and APTES functionalized nanoparticles, only the S and the most appropriate S-APTES nanoparticle were subjected to in vitro release experiments. These studies were carried out using dialysis tubing (Membra-cell MD34, MWDO: 14000 Da) method, in double distilled water with a pH 1.2 at 37°C. Release profiles of the CFD loaded S and S-APTES nanoparticles were plotted in Figure 3.12 using the data given in Table 3.6.

Table 3.6 Data of release experiments.

Time (h)	Amount of CFD released M_t (mg)		Amount of remaining CFD M (mg)		Release of CFD (%)	
	S	S-APTES	S	S-APTES	S	S-APTES
0	0	0	3.23*	2.57*	0	0
2	0.53	0.278	2.70	2.29	16.5	10.8
4	0.43	0.14	2.80	2.42	13.2	5.6
6	0.47	0.29	2.76	2.28	14.4	11.2
8	0.69	0.36	2.54	2.21	21.5	13.9
10	0.74	0.39	2.49	2.18	23.0	15.0
12	0.82	0.39	2.41	2.18	25.5	15.0
24	0.82	0.39	2.41	2.18	25.5	15.0

*Initial amount of drug in dialysis tubing (M_0).

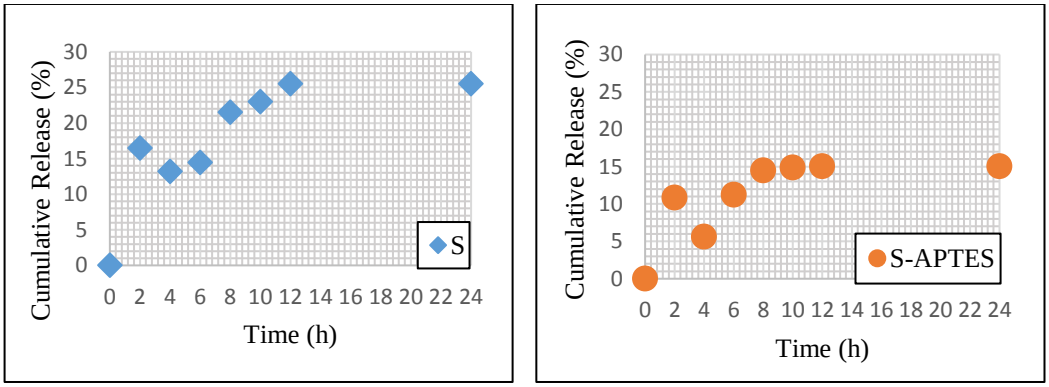

Figure 3.12 Release profiles of CFD loaded S (a) and S-APTES (b) nps (pH 1.2 and 37°C).

The release of CFD was characterized by initial fast release with 16.5% and 10.8% of the total amount of CFD detected during the first 2 hours for S and S-APTES particles, respectively. The reason of this initial fast release was the unloaded CFD molecules that were absorbed on the nanoparticle surface. After 10 hours, almost no CFD released from S-APTES particles and this duration was 12 hours for S particles.

Release experiments were repeated twice. Results of release experiments are listed in Table 3.7.

Table 3.7 Results of release experiments.

Particle	**Release of CFD (%) after 2 h**	**Release of CFD (%) after 10 h**	**Release of CFD (%) after 12 h**	**Release of CFD (%) after 24 h**
S	16.5	23.0	25.5	25.5
S-Aptes	10.8	15.0	15.0	15.0

The release kinetics of CFD loaded S and S-APTES nanoparticles were calculated according to zeroth order and first order. The data for release kinetics of CFD and the plots for the first 8 h are given in Table 3.8.

Table 3.8 Data of release kinetics.

t	**M_0-M**		**ln(M_0/M)**	
	S	**S-APTES**	**S**	**S-APTES**
0	0.00	0.00	0.00	0.00
2	0.32	0.14	0.11	0.09
4	0.41	0.15	0.16	0.04
6	0.49	0.33	0.16	0.12
8	0.69	0.37	0.24	0.17

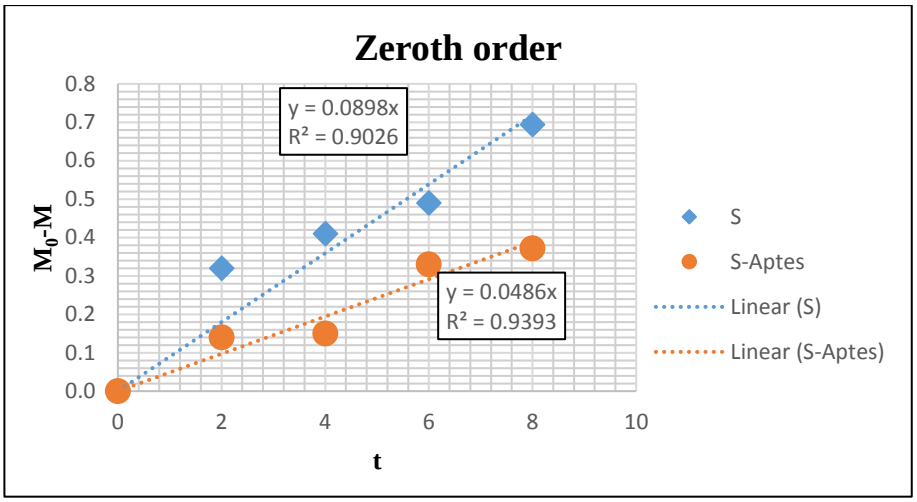

Figure 3.13 Zeroth order kinetics of CFD loaded S and S-APTES nanoparticles.

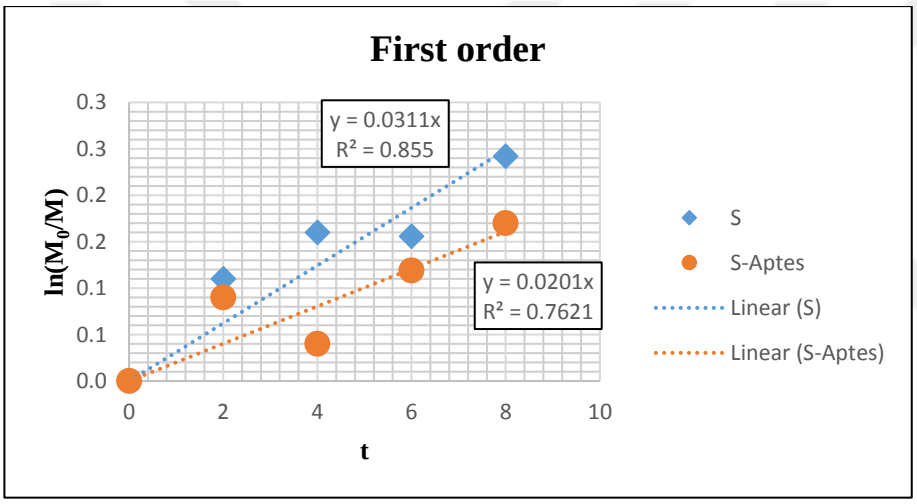

Figure 3.14 First order kinetics of CFD loaded S and S-APTES nanoparticles.

Results of release kinetics of CFD loaded S and S-APTES nanoparticles are given in Table 3.9. As we can see from the regression analysis that Zeroth Order is more fitted to S and S-APTES release profile comparing to First Order. Between S and S-APTES profiles for Zeroth Order, S-APTES shows a better fitting to Zeroth Order Kinetics.

Table 3.9 Results about release kinetics of CFD loaded S and S-Aptes nps.

Particle	Zeroth order		First order	
	k (mg/h)	R^2	k (mg/h)	R^2
S	0.0898	0.9026	0.0311	0.855
S-APTES	0.0486	0.9393	0.0201	0.7621

4. CONCLUSION AND RECOMMENDATIONS

Sodium silicate solutions were prepared from RHA by extraction process and amorphous silica was produced from rice husk by precipitation method successfully. The surfaces of the produced silica were functionalized using Aptes by post-grafting method. The surface functionalized samples were used as drug carriers in drug delivery. All samples had potential for future studies. To conclude:

- Silica particles were functionalized succesfully and the optimum condition was 50°C and n_{APTES}/n_S=0.6 amount the parameters tried. More parameters can be tried to have a better coverage.
- XRD results indicated the synthesis of amorphous SiO_2.
- FTIR result of S particles confirms the presence of Si-O bonds.
- TGA and XPS results show a moderate coverage of silica surface at 50°C and n_{APTES}/n_S=0.6 in functionalization step.
- In contrast to the pure samples, generally after the functionalization the surface area, pore size and pore volume became smaller.
- SEM images gave information about the morphology of the particles.
- TEM images presented the spherical nano S and S-APTES particles.
- The CFD release from S and S-APTES particles was obtained. An initial fast release during 1-2 h and subsequent slow CFD release until 10 h and then a stop in release. The release of CFD from the S nano particles is faster than the S-APTES particles.

For understanding the particle formation mechanism, the structure of silicate solution can be investigated. More parameters can be tried to have a higher coverage of silica surfaces by silane and to explain loading profile. More experiments can be performed to see the repeatibility of the release process better.

REFERENCES

Adam, F., Chew, T.S. and Andas, J., 2011, A simple template-free-sol-gel synthesis of spherical nanosilica from agricultural biomass, J Sol-gel Science Technol 59, 580-583p.

Alshatwi, A.A., Athinarayanan, J. and Periasamy, V.S., 2015, Biocompatibility assessment of rice husk-derived biogenic silica nanoparticles for biomedical applications, Material Science of Engineering 47, 8–16p.

An, D., Guo, Y., Zhu, Y. and Wang, Z., 2010, A green route to preparation of silica powders with rice husk ash and waste gas, Chem. Eng. J. 162, 509-514p.

An, D., Guo, Y., Zou, B., Zhu, Y. and Wang, Z., 2011, A study on the consecutive preparation of silica powders and active carbon from rice husk ash. Biomass Bioenergy 35, 1227-1234p.

Arean, C.O., Vesga, M.J., Parra, J.B. and Delgado, M.R., 2013, Effect of amine and carboxyl functionalization of sub-micrometric MCM-41 spheres on controlled release of cisplatin, Ceramics International 39, 7407-7414p.

Azmi, M.A., Ismail, N.A.A. and Rizamarhaiza, M., 2016, Characterization of silica derived from rice husk (Muar, Johor, Malaysia) decomposition at different temperatures, 2nd Internetional Conference of Functional Material Metal.

Bergna, H.E. and Roberts, W.O., 2006, Colloidal silica: Fundamentals and applications, Boca Raton: Taylor&Frands, 9-37p.

Björkegren, S., Nordstierna, L., Törncrona, A. and Palmvist, A., 2017, Hydrophilic and hydrophobic modifications of colloidal silica particles for pickering emulsions, J Colloid Interface Sci 487, 250-257p.

Carmona, V.B., Oliveira, R.M., Silva, W.T.L., Mattoso, L.H.C. and Marconcini, J.M., 2013, Nanosilica from rice husk: Extraction and characterization, Industrial Crops and Products 43, 291-296p.

Chandrasekhar, S., Satyanarayana, K.G., Pramada, P.N. and Raghavan, P., 2003, Processing, properties and applications od reactive silica from rice husk-an overview, Journal of Material Science 38, 3159-3168p.

REFERENCES (continued)

Chen, S., Chou, P., Chan, W. and Lin, H., 2017, Preparation and characterization of mesoporous bioactive glass from agricultural waste rice husk for targeted anticancer drug delivery, Ceramics International 43, 2239-2246p.

Dash, S., Murthy, N., Nath, L. and Chowdhury, P., 2010, Kinetic modelling on drug release from controlled drug delivery systems, Acta Poloniae Pharmaceutica-Drug Research, 67 3, 217223p.

Demuth, P., Hurley, M., Wu, C., Galanie S., Zachariah, M.R. and Deshong, P., 2011, Mesoscale porous silica as drug delivery vehicles aand pH-sensitive release profiles, Microporous Mesoporous Mater. 141, 128-134p.

Dubey, R.S., Rajesh, Y.B.R.D. and More, M.A., 2015, Synthesis and characterization of SiO_2 nanoparticles via sol-gel method for industrial applications, Materials Today: Proceedings 2, 3575 – 3579p.

Edrissi, M., Soleymani, M. and Adinehnia, M., 2011, Synthesis of silica nanoparticles by ultrasound-assisted sol-gel method: optimized by taguchi robust design, Chemical Engineering Technology 34, 1813-1819p.

Gutowska, A., Jeong, B. and Jasionowski, M., 2001, Injectable gels for tissue engineering, The Anatomical record 263 4.

Herna'ndez, M.S., Herna'ndez, C.S., Fuentes, A.G., Elorza, F., Carrera-Rodri'guez, M. and Alquiza, M.J., 2014, Efficacy from different extraction for chemical profile and biological activities of rice husk, J Sol-Gel Sci Technol 71, 514-521p.

Hieu, N.M., Korobochkin, V.V. and Tu, N.V., 2015, A study of silica separation in the production of activated carbon from rice husk in Viet Nam, Procedia Chemistry 15, 308-312p.

Jal, P.K., Sudarshan, M. and Saha, A., 2004, Synthesis and characterization of nanosilica prepared by precipitation method, Colloids Surf. Physicochem. Eng. Aspect 240, 173-178p.

REFERENCES (continued)

Javed, S., Naveed, S., Feroze, N., Zafar, M. and M. Shafaq, 2010, Crystal and amorphous silica from $KMnO_4$ treated and untreated rice husk, J. Qual. Technol. Manage. 6, 81–90p.

James, J. and Rao, M. S. 1986, Characterization of silica in rice husk ash, Am. Ceram. Soc. Bull. 65, 1177p.

Kalam, S.U., Humayun, M., Parvez, N., Yadav, S., Garg, A., Amin, S., Sultanaand Y. and Ali, A., 2007, Release kinetics of modified pharmaceutical dosage forms: a review, Continental J. Pharmceutical Sciences 1, 30-35p.

Kalu, V.D, Odeniyi, M.A. and Jaiyeoba, K.T, 2007, Matrix properties of a new plant gum in controlled drug delivery, Archieves of Pharmacal Research 30 7, 884-889p.

Kapur, P.C., 1985, Production of reactive bio-silica from the combustion of rice husk in TiB burner, Powder Technol. 44, 63p.

Korsmeyer, R.W., Gurny, R., Doelker, E., Buri, P. and Peppas, N.A, 1983, Mechanisms of solute release from porous hydrophilic polymers, Intrnational Journal of Pharmaceutics 15, 25-35p.

Kortesuo, P., Ahole, M., Karlsson, S., Kangasniemi, I., Yli-Urpo, I. and Kiesvaara, J., 2000, Silica xerogel as an implantable carrier for controlled drug delivery evaluation of drug distribution and tissue effects after implantation, Biomaterials 21 2, 193-198p.

Le, V.H., Nhan, C., Thuc, H. and Thuc, H.H., 2013, Syhthesis of silica nanoparticles from Vietnamese rice husk by sol-gel method. Nanoscale Research Letter 8 1, 58-68p.

Lin, Y.S. and Haynes, C.L., 2009, Synthesis and characterization of biocompatible and size-tunable multifunctional porous silica nanoparticles, Chem. Mater. 21, 3979-3986p.

Liou, T.H., 2004, Preparation and characterization of nanostructured silica from rice husk, Materials Science and Engineering A 364, 313-323p.

REFERENCES (continued)

Liou, T.H. and Yang, C.C., 2011, Synthesis and surface characteristics of nanosilica produced from alkali-extracted rice husk ash. Mater. Sci. Eng. B 176, 521-529p.

Liu, D., Zhang, W., Lin, H., Li, Y., Lu, H. and Wang, Y., 2016, A green technology for the preparation of high capacitance rice husk-based activated carbon, Journal of Cleaner Production 112, 1190-1198p.

Luan, T.C. and Chou, T.C., 1990, Recovery of silica fromt he gasification of rice husk/coal in the presence of a pilot flame in a modified fluidized bed, Ind. Eng. Chem. Res. 29, 1922p.

Manzano, M., Aina, V., Arean, C.O., Balasa, F., Cauda, V., Colilla, M., Delgado, M.R. and Vallet-Regi, M., 2008, Studied on MCM-41 mesoporous silica for drug delivery: effect of particle morphology and amine functionalization, Chem Eng J 137, 30-37p.

Maria, G., Berger, D., Nastase, S. and Luta, I., 2012, Kinetic studies on the irinotecan release based on structural properties of functionalized mesoporous-silica supports, Microporous and Mesoporous Materials 149, 25-35.

Maria, G, Stoica, A., Luta, I., Stirbet, D. and Radu, G., 2012, Cephalosporin release from funcitonalized MCM-41 supports interpreted by various models, Microporous and Mesoporous Materials 162, 80-90p.

Mehta, A. and Ugwekar, R.P., 2015, Extraction of silica and other related products from rice husk, Int. J. Eng. Res. App. 5 8, 2248-9622, 43-48p.

Misran, H., Yarmo, M.A. and Ramesh, S., 2013, Synthesis and characterization of silica nanospheres using nonsurfactant template, Ceramics International 39, 931-940p.

Mor, S., Manchanda, C.K. and Ravindra, K., 2016, Nanosilica extraction from processed agricultural residue using green technology, Journal of Cleaner Production.

REFERENCES (continued)

Nakata, Y., Suzuki, M., Okutani, T., Kikuchi, M. and Akiyama, T., 1989, Prepararion and properties of SiO_2 from rice hulls, J. Ceram. Soc. Jpn. 97, 842p.

Park, S.K., Kim, K.D. and Kim, H.T., 2002, Preparation of silica nanoparticles: determination of the optimal synthesis conditions for small and uniform particles, Colloids and Surfaces A: Physicochemical and Engineering Aspects 197, 7-17p.

Rahman, I. and Padavettan, V., 2012, Sythesis of silica nanoparticles by Sol-Gel: Size dependent properties, surface modification and applications in silica polymer nanocomposites – A review, Journal of Nanomaterials 2012.

Real, C., Alcala, M.D. and Criado, C.M., 1996, Preparation of silica from rice husks, J. Am. Ceram. Soc. 79, 2012–2016p.

Sankar, S., Sharma, S. K. and Kim, D. Y., 2016, Synthesis and characterization of mesoporous SiO_2 nanoparticles synthesized from biogenic rice husk ash for optoelectronic applications, International Journal of Engineering 17.

Selvi, A., and Das, N., 2015, Remediation of cefdinir from aqueous solution using pretreated dead yeast Candida sp. SMN04 as potential adsorbent: an equilibrium, kinetics and thermodynamic studies, Scholars Research Library 7 4, 74-81p.

Shen, J., Liu, X., Zhu, S., Zhang, H. and Tan, J., 2011, Effects of calcination parameters on the silica phase of original and leached rice husk ash, Mater. Lett. 65, 1179–1183p.

Singhvi, G. and Singh, M., 2011, Review: In-vitro drug release characterization models, International Journal of Pharmaceutical Studies and Research 2, 77-84p.

Song, S.W., Hidajat, K. and Kawi, S., Functionalized SBA-15 materials as carriers for controlled drug delivery: Influence of surface properties on Matrix-Drug Interactions, Langmuir 21, 9568-9575p.

REFERENCES (continued)

Stöber, W. and Fink, A., 1968, Controlled growth of monodisperse silica spheres in the micron size range, Journal of Colloid and Interface Science 26, 62-69p.

Szegedi, A., Popova, M., Goshev, I. and Mihaly, J., 2011, Effect of amin functionalization of spherical MCM-41 and SBA-15 on controlled drug release, J Solid Stat Chem 184, 1201-1207p.

Thuadaij, N. and Nuntiya A., 2008, Preparation of nanosilica powder from rice husk ash by precipitation method. Chiang Mai J. Sci. 35 1, 206-211p.

Tolba, G.M.K., Barakat, N.A.M., Bastaweesy, A.M., Ashour, E.A., Abdelmoez, W., El-Newehy, M.H., Al-Deyab, S.S. and Kim, H.Y., 2015, Effective and highly recyclable nanosilica produced from the rice husk for effective removal of organic dyes, J. Ind. Eng. Chem. 29, 134–145p.

Trewyn, B.G, Nieweg, J.A., Zhao, Y. and Lin, V.S.Y., 2008, Biocompatible silica nanoparticles with different morphologies for animal cell membrane penetration, Chemical Engineering Journal 137, 23-29p.

Vaibhav, V., Vijayalakhmi, U. and Roopan, S.M, 2014, Agricultural waste as a source for the production of silica nanoparticles, Spectrochimica Acta Part A: Molecular and Biomolecular Spectroscopy 139, 515-520p.

Wang, N. and Low, M.J.D., 1990, Spectroscopic studies of carbons XVIII: The charring of rice hulls, Mater. Chem. Phys. 26, 117p.

Xiong, L., Sekia, E.H., Sujaridworakun, P., Wada, S., and Saito, K., 2009, Burning temperature dependence of rice husk ashes in structure and property, J. Metals Mater. Miner. 19, 95–99p.

Yener, H.B. and Helvacı, Ş.Ş., 2015, Effect of synthesis temperature on the structural properties and photocatalytic activity of TiO_2/SiO_2 composites synthesized using rice husk ash as a SiO_2 source, Separation and Purification Technology 140, 84-93p.

Yılmaz, M.S, Palantoken, A. and Piskin, S., 2016, Release of flurbiprofen using of SBA-15 mesoporous silica: Influence of silica source and functionalization, Journal of non-crystalline solids 437, 80-86p.

REFERENCES (continued)

Yoo, Y., Shin, H.W. and Nam, B.G., 2003, Effect of hydrophilic-lipophilic balance of drugs on their release behavior from amphiphilic matrix, Macromolecular Research 11 4, 283-290p.

Yuvakkumar, R., Elango, V., Rajendran, V. and Kannan, N., 2014, High-purity nano silica powder from rice husk using a simple chemical method, Journal of Experimental Nanoscience 9 3, 272-281p.

Zhang, Y., Zhuangzhi, Z., Jiang, T., Zhang, J., Wang, Z. and Wang, S., 2010, Spherical mesoporous silica nanoparticles for loading and release of the

poorly water-soluble drug telmisartan, Journal of Controlled Release 145, 257-263p.

Zulfiqar, U., Subhani, S.W and Husain, S.W, 2015, Synthesis of silica nanoparticles from soduim silicate under alkaline conditions, J Sol-Gel Technol 77, 753-758p.

Zulkifli, N.SC., Ab Rahman, I., Mohamed, D. and Husein, A., 2013, A green sol-gel route for the synthesis of structurally controlled silica particles from rice husk for dental composite filler. Ceram. Int. 39, 4559-4567p.

ACKNOWLEDGEMENT

I would like to extend my sincerest gratitude towards my research supervisor Prof. Dr. Şerife Şeref HELVACI for her valuable guidance through her MSc studies. I express my thankfulness to my advisor Res. Assist. Dr. H. Banu YENER for her support during the thesis. My sincere thanks also goes to my fellow lab mates Gizem TUFANER and Pelin ÖZ for stimulating discussions during the all year.

This work was supported by the Ministry of Education, Youth and Sports of the Czech Republic Program NPU I (LO1504). The XRD data was measured due to the support of Operational Program Research and Development for Innovations co-funded by the European Regional Development Fund (ERDF) and national budget of the Czech Republic, within the framework of the project CPS strengthening research capacity (reg. number: CZ.1.05/2.1.00/19.0409). Thanks to Prof. Dr. Vladimír SEDLAŘÍK for his guidance during period in Czech Republic and also allowing me to use all the devices/equipments I needed in the laboratories.

I would also like to thank Erdoğanlar Food Industry and Kansai Altan Paint Industry and Trade Incorporation for supplying rice husk ash and APTES, respectively, required for the experiments.

Lastly, I am deeply indebted to my father Erdoğan ÇALIŞKAN, mother Belkıs ÇALIŞKAN and dear Alper ÖZCEL who provided me the greatest support and encouragement.

CURRICULUM VITAE

Contact information :

Açelya Çalışkan

İzmir, Karşıyaka, Örnekköy Mah., 7539 Sokak, No:5/1

+90 539 889 6029 / +90 535 946 3651

caliskanacelya@hotmail.com

TR – Female - 12/06/1990

Education :

2016-2019	Graduate	Ege Uni.	Turkey	Chemical Eng.	3.6/4
2008-2015	Bachelor	Ege Uni.	Turkey	Chemical Eng.	2.6/4
2011-2012	Bachelor	Porto Uni.	Portugal	Chemical Eng.	LLP
2004-2008	High school	Atakent Anatolian	Turkey	Science	95/100

Language skills :

Turkish	Native
English	Advanced
German	Intermediate

Computer skills :

Microsoft Office	Excellent
Matlab	Intermediate
Intellicad	Intermediate

Experience :

2019	Molkim	R&D Engineer	8 m
2018	Tomas Bata University in Zlín	Temporary Project Officer	6 m
2012	Maxion Wheels	Intern Engineer	2 m
2010	İnci GS Yuasa	Intern Engineer	2 m

Seminars and courses :

2011	Creative Drama	TEGV	144 h
2011	Portuguese Language	Porto University	60 h
2010	German Language	Tömer	384 h

Scholarships :

2016-2018 Cevdet İnci Educational Foundation – Success scholarship

2008-2013 Cevdet İnci Educational Foundation – Success scholarship

Projects and presentations :

2018 'Calcination method in the presence of activating chemicals: effective parameters in silica production from rice husk ash', 13th National Congress of Chemical Engineering (oral ppt)

2013 'Stability and release behavior of drug loaded nanoemulsions' Advanced Materials World Congress (oral ppt)

2009-2010 1th UKMOP (National Student Platform of Chemical Engineering). My mission was finding expert academicians, public and firm representatives to make presentations on the platform.

Interests : Discovering science, psychology, spiritual awakening, exploring new cultures

Memberships : KMO, TEGV

References : Didem Tunç, Senior Quality Engineer at Hayat Chemicals
ditunc@hayat.com.tr (+90 536 968 69 99)
Prof. Dr. Şerife Şeref Helvacı, Ege University Chemical Engineering Department
sshelvaci@gmail.com (+90 544 576 38 06)

APPENDIX

Method of silanation

The amount of silica (S) for each experiment (g): 3

The weight percentage of S in alcogel (w %): 8.25

The amount of alcogel required (g):

$$3\text{g} * \frac{100}{8.25} = 36.3636 \text{ g alcogel}$$

Parameters: T and n_{APTES}/n_S

Calculation of the amount of solvent (ethanol) (for 3% EtOH solution):

$$\frac{3\text{g S}}{\text{xg EtOH}} = 0.03 \rightarrow \text{x} = 100\text{gEtOH}$$

$$V_{EtOH} = 100\text{g} * \frac{\text{mol}}{0.789\text{gEtOH}} \sim 130\text{mL}$$

Calculation of the amount of APTES:

$$n_S = \frac{3\text{g}}{60\frac{\text{g}}{\text{mol}}} = 0.05\text{mol}$$

For $n_{APTES}/n_S=0.2$: $\frac{n_{APTES}}{n_S} = 0.2 \rightarrow \frac{n_{APTES}}{0.05 \text{ mol}} = 0.2 \rightarrow n_{APTES} = 0.01 \text{ mol}$

$$V_{APTES} = 0.01 \text{ mol} * \frac{\text{mL}}{0.946\text{g}} * \frac{221.372 \text{ g}}{\text{mol}} = 2.34 \text{ mL}$$

For $n_{APTES}/n_S=0.4$: $\frac{n_{APTES}}{n_S} = 0.4 \rightarrow \frac{n_{APTES}}{0.05 \text{ mol}} = 0.4 \rightarrow n_{APTES} = 0.02 \text{ mol}$

$$V_{APTES} = 4.68 \text{ mL}$$

$$\underline{\text{For } n_{APTES}/n_S=0.6}: \frac{n_{APTES}}{n_S} = 0.6 \rightarrow \frac{n_{APTES}}{0.05\ \text{mol}} = 0.6 \rightarrow n_{Aptes} = 0.03\ \text{mol}$$

$$V_{APTES} = 7.02\ \text{mL}$$